Exactly solvable floquet dynamics for conformal field theories in dimensions greater than two

Diptarka Das [a] **Sumit R. Das** [b] **Arnab Kundu** [c,d] **and Krishnendu Sengupta** [e]

[a]*Department of Physics, Indian Institute of Technology, Kanpur,*
UP 208016, India

[b]*Department of Physics and Astronomy, University of Kentucky,*
Lexington, KY 40506, U.S.A.

[c]*Saha Institute of Nuclear Physics, 1/AF Bidhannagar,*
Kolkata 700064, India

[d]*Homi Bhaba National Institute, Training School Complex, Anushaktinagar,*
Mumbai 400094, India

[e]*School of Physical Sciences, Indian Association for the Cultivation of Science,*
Jadavpur, Kolkata 700032, India

E-mail: didas@iitk.ac.in, das@pa.uky.edu, arnab.kundu@saha.ac.in,
tpks@iacs.res.in

ABSTRACT: We find classes of driven conformal field theories (CFT) in $d+1$ dimensions with $d > 1$, whose quench and floquet dynamics can be computed exactly. The setup is suitable for studying periodic drives, consisting of square pulse protocols for which Hamiltonian evolution takes place with different deformations of the original CFT Hamiltonian in successive time intervals. These deformations are realized by specific combinations of conformal generators with a deformation parameter β; the $\beta < 1$ ($\beta > 1$) Hamiltonians can be unitarily related to the standard (Lüscher-Mack) CFT Hamiltonians. The resulting time evolution can be then calculated by performing appropriate conformal transformations. For $d \leq 3$ we show that the transformations can be easily obtained in a quaternion formalism. Evolution with such a single Hamiltonian yields qualitatively different time dependences of observables depending on the value of β, with exponential decays characteristic of heating for $\beta > 1$, oscillations for $\beta < 1$ and power law decays for $\beta = 1$. This manifests itself in the behavior of the fidelity, unequal-time correlator, and the energy density at the end of a single cycle of a square pulse protocol with different hamiltonians in successive time intervals. When the Hamiltonians in a cycle involve generators of a single $\mathrm{SU}(1,1)$ subalgebra we calculate the Floquet Hamiltonian. We show that one can get dynamical phase transitions for any β by varying the time period of a cycle, where the system can go from a non-heating phase which is oscillatory as a function of the time period to a heating phase with an exponentially damped behavior. Our methods can be generalized to other discrete and continuous protocols. We also point out that our results are expected to hold for a broader class of QFTs that possesses an $\mathrm{SL}(2, C)$ symmetry with fields that transform as quasi-primaries under this. As an example, we briefly comment on celestial CFTs in this context.

Contents

1 Introduction

The study of time evolution of a driven quantum system with a time dependent Hamiltonian is a valuable tool for gaining insight into its non-equilibrium properties. Useful drive protocols include quantum quench, ramp, and periodic or quasi-periodic drive protocols [1–4]. Recently, properties of quantum systems driven via periodic protocols have been most intensely studied; such systems undergo evolution governed by Hamiltonian periodic in time with a time period T. Interestingly, at strobosocopic times $t = nT$, where n is an integer, the evolution operators of such systems can be written as $U(nT, 0) = \exp[-iH_F nT]$; the corresponding dynamics is then completely controlled by the Floquet Hamiltonian H_F.

However, most of these studies require numerical work: analytically tractable models are limited to free field theories or two dimensional conformal field theories. For the latter class of theories, the underlying infinite dimensional symmetry algebra provides a powerful tool to calculate physical quantities of interest. One example involves a sudden quench from a massive theory to a two dimensional CFT whose IR properties can be well approximated by a Cardy-Calabrese state [5], and the time evolution can be calculated by using conformal

mapping. A more recent example involves quench and Floquet dynamics in a two dimensional CFT [6–16]: once again the time evolution can be obtained by conformal maps. No such analytical results are known in higher dimensions, and one has to typically resort to numerical calculations which are often limited by finite size effects.[1]

In this paper we demonstrate that a class of time dependent problems can be exactly studied in conformal field theories in *arbitrary number of dimensions* and lead to interesting non-trivial dynamics. Our work is inspired by the work of [6] who studied a $1+1$ dimensional CFT on a strip which starts from the usual CFT Hamiltonian and is quenched by a sine squared deformed (SSD) one. The SSD-CFT$_2$ has been studied previously in [17–21]. Both these Hamiltonians belong to the global part of the Virasoro algebra. The time evolution then becomes a Möbius transformation. The global part of the Virasoro algebra is (in Euclidean signature) SO(3,1) (generated by $L_0, L_{\pm 1}$ and their hermitian conjugates). Floquet generalizations to periodically driven CFTs by a sequence of the usual CFT Hamiltonian and SSD Hamiltonian for successive time durations T_i were studied in [12, 14, 16]. Generalizations of the SSD to other SL_2 subgroups of Virasoro were studied in [15]. Holographic interpretations were investigated in [7–9, 11] and from a different perspective in [22].

In higher dimensions $(d+1)$, the conformal algebra is $SO(d+2,1)$. This suggests that a natural generalization to higher dimensional systems can be obtained by considering different generators of the conformal algebra as Hamiltonians and considering sequences of non-commuting Hamiltonians in successive time intervals. Similar to the two dimensional case, the dynamics is expected to be equivalent to conformal transformations.

In this work we consider conformal field theories on $S^d \times$ time. The class of Hamiltonians are combinations of generators which belong to $SL(2,R) \sim SU(1,1)$ subrgoups of the conformal group. More specifically we consider

$$H(\beta, \Pi) = 2iD + i\beta(K_\mu + P_\mu)\Pi^\mu \,, \tag{1.1}$$

where the operators D, K_μ, P_μ $(\mu, \nu = 0, \cdots d)$ are generators of conformal transformations (see below) and Π^μ is a projector along μ-direction (e.g. $\Pi^0 = (1, 0, 0, \dots)$). In the field theory Hilbert space the hermiticity properties of these generators are

$$D^\dagger = -D \qquad K_\mu^\dagger = -P_\mu \tag{1.2}$$

black Note that there are $(d+1)$ such different $SL(2,R)$ subalgebras corresponding to $(d+1)$-inequivalent choices of Π^μ. This provides a wider class of drive protocols where one can use different members of the class of Hamiltonians $H(\beta, \Pi)$, for different time intervals. In the latter case, the net transformation is not a $SU(1,1)$ transformation.

In terms of the energy momentum tensor, the Hamiltonian on $S^d \times$ (time) may be written as

$$H(\beta, \Pi) = 2 \int d\Omega_d \left[1 + \frac{1}{2}\beta Y_\mu \Pi^\mu \right] T_{ww} \tag{1.3}$$

where Y^μ denote cartesian coordinates on a R^{d+1}, where the sphere S^d is the surface $Y^\mu Y_\mu = 1$, $d\Omega_d$ denotes the volume element on S^d and w denotes the Euclidean time.

---

[1] A different class of problems involving fast smooth quenches in conformal field theories in arbitrary dimension can be addressed using conformal properties [23, 24].

As will be shown below, when $\beta < 1$ a Hamiltonian of the form (1.1) can be transformed to the standard CFT Hamiltonian ($H_{\mathrm{ST}} = 2iD$) (on the plane), while for $\beta > 1$ it can be transformed to the Lüscher-Mack (LM) type Hamiltonian ($H_{\mathrm{LM}} = i(P_\mu + K_\mu)$). We note that for a CFT on S^d, H_{LM} shares the same vacuum as the H_{ST}. However as we shall show, the two Hamiltonians are related by a non-unitary transformation. Furthermore unitary time evolution with H_{LM} results in exponential time dependence.

As is standard in CFT's, it is convenient to first work in Euclidean signature and perform a Weyl transformation to a plane R^{d+1}

$$ds^2 = dw^2 + d\Omega_d^2 = \frac{1}{r^2}\left[\delta_{\mu\nu}dx^\mu dx^\nu\right] \tag{1.4}$$

where x^μ are cartesian coordinates on R^{d+1} and

$$r^2 = \delta_{\mu\nu}x^\mu x^\nu = e^w. \tag{1.5}$$

The operator ($2iD$) becomes the dilatation operator on the plane, while P_μ generates translations on the plane. Acting on functions on R^{d+1} the conformal generators are represented by the following differential operators

$$D = -ix_\mu\partial_\mu, \quad P_\mu = -i\partial_\mu, \quad K_\mu = -i(2x_\mu(x_\nu\partial_\nu) - r^2\partial_\mu),$$
$$L_{\mu\nu} = -i(x_\mu\partial_\nu - x_\nu\partial_\mu). \tag{1.6}$$

For a fixed μ the generators D, P_μ, K_μ form an $SU(1,1)$ subalgebra of the Euclidean conformal algebra $SO(d+2,1)$. There are $d+1$ such subgroups corresponding to different choice of μ. The $SU(1,1)$ nature of these subgroups can be understood by noting that the commutation of these generators satisfy

$$[D, K_\mu] = -iK_\mu, \quad [D, P_\mu] = iP_\mu, \quad [K_\mu, P_\mu] = 2iD. \tag{1.7}$$

Our strategy for calculating the response is analogous to the earlier works in $1+1$ dimensions. We will perform a Weyl transformation to R^{d+1}, where the expressions for the generators and the resulting conformal transformation become simple, calculate the time evolution by evaluating the corresponding conformal transformation, transform back to $S^d \times$ time and finally continue to real time. While this is straightforward in principle, this becomes quickly cumbersome in practice for $d > 1$.

The key technical tool which facilitates our calculations is the fact that when $d \leq 3$, a point on R^{d+1} can be represented by a quaternion and the action of finite conformal transformations take a simple form, generalizing Möbius transformations on the complex plane to Möbius transformations on the field of quaternions, $SL(2,H)$. In general, the parameters of these transformations are themselves quaternions. However, when the transformation belongs to an $SL(2,R)$ subgroup of the conformal group one can judiciously choose the quaternion representation such that these parameters become real numbers. When continued to real time, these transformations are represented by $SU(1,1)$ transformations on quaternions and correspond to real transformations of the coordinates While this simplifies our calculations considerably, this necessitates switching quaternionic representations whenever we switch

from one $\mathrm{SL}(2, R)$ subgroup to another. It should be emphasized that when a cycle involves different $\mathrm{SL}(2, R) \sim \mathrm{SU}(1, 1)$ subgroups the net transformation is not a $\mathrm{SL}(2, R) \sim \mathrm{SU}(1, 1)$ transformation. This is then essentially different from the $d = 1$ case investigated in the literature. In this work, we provide explicit results for $3 + 1$ dimensions, though it should be emphasized that the framework is completely general for any $d \leq 3$.

In the following we first consider properties of various quantities after a single drive cycle as a function of the time period T of the drive and β. Each cycle involves Hamiltonians of the form (1.1) with various $\Pi^\mu, \mu = 0, 1, \cdots 3$ for successive time intervals of *equal* value. The value of β is either zero, or some fixed value, i.e. we do not consider different non-zero values of β for different time intervals. These restrictions are for simplicity. All these diagonistics show that for $\beta < 1$ the response is oscillatory as a function of the time period, while for $\beta > 1$ one exponential decays for large time period. $\beta = 1$ is a critical value, where the quantities have power law behavior. Since the driving Hamiltonians break rotation invariance on the S^d the system develops inhomogenities. The nature of the inhomogeneties is richer in these higher dimensional cases, since we have the ability to break different sets of symmetries by choosing different sequences of $H_1 \cdots H_{d+1}$. It can be easily seen that if we use different nonzero values of β the behavior is oscillatory when all the β values are less than 1, power law when all the β are equal to one. If any of the β exceed 1, the behavior will be exponential.

When all the hamiltonians in a cycle belong to the same $\mathrm{SU}(1, 1)$ subgroup of the conformal group, we calculate the Floquet hamiltonian explicitly, so that the behavior after an arbitrary number of cycles, n, can be then read off easily. We show that the three conjugacy classes of $\mathrm{SU}(1, 1)$ correspond to exponential, oscillatory and power law behaviors as a function of the number of cycles, n. By changing the time intervals inside a single cycle we show that one can make transitions between these different phases both for $\beta < 1$ and $\beta > 1$.

When the cycles involve different Mobius subgroups, one needs to look at conjugacy classes of $\mathrm{SL}(2, H)$. We indicate how one can proceed in this general case, but defer a detailed investigation to a future publication.

The plan of the rest of this work is as follows. In section 2 we study the properties of Hamiltonians of the form (1.1). This is followed by section 3 which deals with our strategy for calculating the response to the dynamics for general d and the formulation in terms of quaternions for $d = 3$. Next, in section 4, we provide results for three quantities under the dynamics. The first corresponds to the fidelity of an evolving primary state at the end of a drive cycle; this is discussed in subsection 4.1. The second constitutes behavior of unequal-time correlation functions of the CFT under such evolution; this is discussed subsection 4.2. The evolution of the stress tensor, starting from a primary CFT state, is discussed in subsection 4.3. As expected, the conformal anomaly plays a role in this calculation. In section E we find the fixed points and fixed surfaces for quaternionic Möbius transformations which belong to a single $\mathrm{SU}(1, 1)$ and determine the trajectories of points under successive cycles of a periodic drive. Finally, we discuss our main results and conclude in section 5. Some details of the calculation are provided in the appendix.

2 The deformed CFTs

In this section we will discuss some properties of deformed CFT's with a Hamiltonian of the form (1.1).

2.1 $\beta < 1$ and Möbius quantization

When $\beta < 1$, for the choice e.g. $\Pi^\mu = (1,0,0,0)$, the Hamiltonian H (defined in (1.1)) can be thought of a different quantization of the theory with the undeformed hamitonian ($\beta = 0$) upto a scaling of the new time. For $d = 1$ this has been called "Möbius quantization". Consider the Hamiltonian

$$\tilde{H} = \frac{1}{\sqrt{1-\beta^2}} H = (\cosh\theta)2iD + i(\sinh\theta)(K_0 + P_0) \qquad \beta = \tanh\theta \,. \tag{2.1}$$

This Hamiltonian is related to the dilatation operator by a similarity transformation

$$U^{-1}\tilde{H}U = (2iD), \quad U = \exp\left[-\frac{i}{2}\theta(K_0 - P_0)\right] \,. \tag{2.2}$$

This can be verified by explicit calculation. However since the left hand side of (2.2) depends only on the commutators of the generators of the $SU(1,1)$ group, the equation must be independent of the specific representation.

To verify (2.2) it is convenient to use a representation of the $SU(1,1)$ using Pauli matrices,

$$D = i\sigma_z/2, \quad K_0 = \sigma_-, \quad P_0 = \sigma_+ \quad \sigma_\pm = \frac{1}{2}(\sigma_x \pm i\sigma_y). \tag{2.3}$$

The transformed special conformal and translation generators can be now deduced using the identities

$$\begin{aligned}
U^{-1}\sigma_z U &\equiv \tau_z = \sigma_z \cosh\theta + i\sigma_x \sinh\theta \\
U^{-1}\sigma_x U &\equiv \tau_x = \sigma_x \cosh\theta - i\sigma_z \sinh\theta, \quad \tau_y = \sigma_y \,.
\end{aligned} \tag{2.4}$$

Using the representation (2.3) this leads to

$$\begin{aligned}
U^{-1}DU &= D\cosh\theta + \frac{1}{2}(K_0 + P_0)\sinh\theta \\
U^{-1}K_0 U &= \frac{1}{2}(1+\cosh\theta)K_0 - \frac{1}{2}(1-\cosh\theta)P_0 - D\sinh\theta \,, \\
U^{-1}P_0 U &= \frac{1}{2}(1+\cosh\theta)P_0 - \frac{1}{2}(1-\cosh\theta)K_0 - D\sinh\theta \,.
\end{aligned} \tag{2.5}$$

To calculate the transformation of the other generators of the conformal algebra, it is useful to consider the combinations

$$A_\mu \equiv \frac{1}{2}(K_\mu - P_\mu) \qquad B_\mu \equiv \frac{1}{2}(K_\mu + P_\mu) \,. \tag{2.6}$$

The conformal algebra then leads to a closed $SL(2,R)$ subalgebra for the generators (A_0, A_j, L_{0j}) for each value of $j = 1,2,3$

$$[A_0, L_{0j}] = iA_j \qquad [A_0, A_j] = iL_{0j} \qquad [L_{0j}, A_j] = iA_0 \,. \tag{2.7}$$

Now consider the transformed A_j or L_{0j} (these angular momentum generators are defined in (1.6)),

$$U^{-1}A_j U = e^{i\theta A_0} A_j e^{-i\theta A_0} \qquad U^{-1}L_{0j} U = e^{i\theta A_0} L_{0j} e^{-i\theta A_0} \tag{2.8}$$

Once again, the result is determined entirely in terms of commutators. We can therefore use any representation of the algebra (2.7) to perform the calculation, e.g. the representation in terms of Pauli matrices

$$L_{0j} \to \frac{1}{2}\sigma_x \quad A_j \to \frac{1}{2}i\sigma_z \quad A_0 \to -\frac{1}{2}i\sigma_y \tag{2.9}$$

to obtain

$$U^{-1}A_jU = A_j \cosh\theta - L_{0j}\sinh\theta$$
$$U^{-1}L_{0j}U = L_{0j}\cosh\theta - A_j\sinh\theta\,. \tag{2.10}$$

Furthermore the conformal algebra implies

$$[A_0, K_j + P_j] = [A_0, L_{ij}] = 0\,. \tag{2.11}$$

This leads to final form of the deformed generators:

$$U^{-1}DU = D\cosh\theta - \frac{1}{2}(K_0 + P_0)\sinh\theta$$

$$U^{-1}K_0U = \frac{1}{2}(1 + \cosh\theta)K_0 - \frac{1}{2}(1 - \cosh\theta)P_0 - D\sinh\theta$$

$$U^{-1}P_0U = \frac{1}{2}(1 + \cosh\theta)P_0 - \frac{1}{2}(1 - \cosh\theta)K_0 - D\sinh\theta$$

$$U^{-1}K_jU = \frac{1}{2}(1 + \cosh\theta)K_j + \frac{1}{2}(1 - \cosh\theta)P_j - L_{0j}\sinh\theta$$

$$U^{-1}P_jU = \frac{1}{2}(1 + \cosh\theta)P_j + \frac{1}{2}(1 - \cosh\theta)K_j + L_{0j}\sinh\theta$$

$$U^{-1}L_{0j}U = \cosh\theta\, L_{0j} + \frac{1}{2}\sinh\theta(P_j - K_j), \quad U^{-1}L_{ij}U = L_{ij}\,. \tag{2.12}$$

These relations can be alternatively derived by first looking at the coordinate transformations resulting from the action of U with infinitesimal θ, and exponentiating them and requiring that the correct commutation relations are satisfied by the deformed generators. This is detailed in the appendix.

The results of this subsection imply that for $\beta < 1$ the deformed Hamiltonian is proportional to a standard CFT Hamiltonian (dilatation operator) which is quantized with a different notion of time. Consequently aspects of the physics of the deformed Hamiltonian are expected to be qualitatively similar to the undeformed Hamiltonian.

2.2 $\beta > 1$ and Lüscher-Mack Hamiltonians

The unitary transformation which relates the deformed theory to the undeformed theory for $\beta < 1$ does not work when $\beta > 1$. We will now demonstrate that for $\beta > 1$ the Hamiltonian can be instead deformed to the generator $K_0 + P_0$. Consider the Hamiltonian

$$\hat{H} = \frac{1}{\sqrt{\beta^2 - 1}}H = 2iD\sinh\phi + i(K_0 + P_0)\cosh\phi \quad \beta = \coth\phi\,. \tag{2.13}$$

Using manipulations entirely similar to the previous subsection it is easy to show that

$$U^{-1}\hat{H}U = i(K_0 + P_0), \quad U = \exp\left[-\frac{i}{2}\phi(K_0 - P_0)\right]\,. \tag{2.14}$$

The transformations of the other generators can be worked out following a procedure entirely analogous to the previous subsection. This shows that the physics of the deformed theory for $\beta > 1$ is similar to a theory with a Lüscher-Mack Hamiltonian $H_{LM} = \frac{i}{2}(K_0 + P_0)$ rather than the dilatation operator. In fact one has the following relationship:

$$\frac{i}{2}(K + P) = e^{\frac{\pi}{4}(K-P)} D e^{-\frac{\pi}{4}(K-P)}. \tag{2.15}$$

If we let $|\tilde{\Delta}_n\rangle$ be the eigenstate of D, i.e. $D|\tilde{\Delta}_n\rangle = \tilde{\Delta}_n|\tilde{\Delta}_n\rangle$ (with $\tilde{\Delta}_n = i\mathbb{R}$), then one can define left and right eigenvectors of LM Hamiltonian:

$$|n_r\rangle = e^{\frac{\pi}{4}(K-P)}|\tilde{\Delta}_n\rangle, \ \ \langle n_\ell| = \langle \tilde{\Delta}_n|e^{-\frac{\pi}{4}(K-P)}. \tag{2.16}$$

These states satisfy: $\langle n_\ell|n'_r\rangle = \delta_{\tilde{\Delta}_n, \tilde{\Delta}'_n}$ and, $\sum_n |n_r\rangle\langle n_\ell| = \mathbb{I}$. This construction is similar to the one recently used in [25]. If we consider the thermal partition function of the LM theory at temperature T, which is: $Z_{LM}(T) = \text{Tr}\, e^{-\frac{i}{2T}(K+P)}$, we may use the above eigenstates to show that this is given by $\text{Tr}\, e^{-\frac{i}{T}(iD)}$. Hence finite temperature for LM theory gets Wick-rotated into imaginary temperature partition function of the standard CFT:

$$Z_{LM}(T) = Z_{CFT}(-iT). \tag{2.17}$$

This is suggestive of the fact that if we look at real time evolution in LM, we may have thermal like behaviours marked by exponential dependence in real time. This we can confirm using the 2×2 representations eq. (2.3). The unitary evolution operator $U(t)$ takes the form:

$$U(t) = \exp\left(-itH_{LM}\right) = e^{\frac{t}{2}\sigma_x} = \begin{pmatrix} \cosh\frac{t}{2} & \sinh\frac{t}{2} \\ \sinh\frac{t}{2} & \cosh\frac{t}{2} \end{pmatrix}. \tag{2.18}$$

As we will see, this difference manifests in dynamical processes like quantum quench by the appearance of a heating phase for $\beta > 1$ and an oscillating phase for $\beta < 1$.

3 Dynamics as a conformal transformation

As mentioned above, it is convenient to think of the time evolution by Hamiltonians like (1.1) by first performing a Weyl transformation to R^{d+1} using eqs. (1.4) and (1.5). Euclidean time evolution with the Hamiltonian $H(\beta, \Pi)$ is equivalent to a conformal transformation. This transformation can be obtained by using the Baker-Campbell-Hausdorff formula [26]

$$U_\mu \Pi^\mu \equiv U(\Pi) = e^{-(2iwD + iw\beta(P_\mu + K_\mu)\Pi^\mu)} = e^{\Lambda_+ K_\mu \Pi^\mu} e^{\ln\Lambda_0 iD/2} e^{\Lambda_- P_\mu \Pi^\mu}$$

$$\Lambda_0 = \left(\cosh w\nu_0 - (w\nu_0)^{-1}\sinh w\nu_0\right)^{-2},$$

$$\Lambda_+ = -\Lambda_- = i\beta\nu_0^{-1}\sinh(w\nu_0)\Lambda_0^{1/2} \tag{3.1}$$

where we have defined

$$\nu_0 = \sqrt{1 - \beta^2} \tag{3.2}$$

To write down the explicit transformations, we separate out the components. For example, using the above relations, one obtains:

$$e^{\alpha_1 iD} x_\nu e^{-\alpha_1 iD} = e^{\alpha_1} x_\nu, \quad e^{i\alpha_2 P_\mu} x_\nu e^{-i\alpha_2 P_\mu} = x_\nu + \alpha_2 \hat{x}_\mu,$$

$$e^{i\alpha_3 K_\mu} x_\nu e^{-i\alpha_3 K_\mu} = \frac{x_\nu}{1 - 2\alpha_3 x_\mu + r^2 \alpha_3^2}, \tag{3.3}$$

where K_μ and x_μ denote the μ-th component of the corresponding vectors.[2] Identifying $\alpha_1 = (1/2)\ln\Lambda_0$, $\alpha_2 = -i\Lambda_-$, and $\alpha_3 = -i\Lambda_+$, we find, after a few lines of algebra and for $\nu \neq \mu$

$$x'_\nu = \frac{x_\nu}{\mathcal{D}_\mu}, \tag{3.4}$$

where the denominator, $\mathcal{D}_\mu = \Big[\Big(\cosh w\nu_0 - (w\nu_0)^{-1}\sinh w\nu_0\Big)^2 + 2x_\mu\beta\nu_0^{-1}\sinh w\nu_0$

$$\times \Big(\cosh w\nu_0 - (w\nu_0)^{-1}\sinh w\nu_0\Big) + \beta^2 r^2 (w\nu_0)^{-2}\sinh^2\tau\nu_0\Big].$$

A similar, but more complicated expression can be obtained for $\nu = \mu$ in a similar manner. One obtains

$$x'_\mu = \Big[x_\mu(2(\cosh^2 w\nu_0 - (w\nu_0)^{-2}\sinh^2 w\nu_0) - 1) - \beta\nu_0^{-1}\sinh w\nu_0(\cosh w\nu_0(1 - r^2)$$

$$- (w\nu_0)^{-1}\sinh w\nu_0(1 + r^2))\Big]/\mathcal{D}_\mu. \tag{3.5}$$

These finite conformal transformations can be then used to express time evolved quantities in terms of the quantities at initial time for any d.

3.1 $d = 3$ and quaternions

In $d \leq 3$ dimensions in general an efficient way to compute the transformed coordinates under the SU$(1,1)$ subgroup of conformal transformations is to use the quaternion formulation. In what follows, we provide details this formulation for $d = 3 + 1$. In Euclidean signature the coordinates are denoted by X^μ with $x_0 = \tau$, $x_1 = x$ and so on. We shall also define the 2×2 matrices $\tau_0 = I$ and $\tau_j = -i\sigma_j$ where σ_j are the standard Pauli matrices and I denotes the identity matrix. The first step of using the quaternion formulation is then to write the coordinates x_μ using a 2×2 matrix by associating each component of the coordinate to one of the τ_μ, where $\vec{\tau} = (I, -i\sigma_j)$, for $j = 1, 2, 3$:

$$Q_\nu = Ix_\nu - i\sum_{j=1}^{3}\sigma_j y_j. \tag{3.6}$$

The y_j which appears here are the components of x^μ with $\mu \neq \nu$. The choice of ν and μ is arbitrary at this stage. As an example, we may choose $\nu = 1$. The three other coordinates x^j which appear are $y_1 = x_0 = \tau, y_2 = x_2 = y, y_3 = x_3 = z$, leading to

$$Q_1 = \begin{pmatrix} x - iz & -i(\tau - iy) \\ -i(\tau + iy) & x + iz \end{pmatrix} \tag{3.7}$$

---

[2]To present these formulae in a completely covariant form, one needs to implement an appropriate projection operator, which we do not use here. Our notation therefore breaks covariance. Nonetheless, we hope it is clear from the context whether we are referring to a vector or a particular component of it.

Clearly Q_ν is not unique even after we fix ν and associate x_ν with the identity matrix since there is freedom of associating the rest of the coordinates with other Pauli matrices in different ways. All such choices lead to identical results for final coordinates under the class of conformal transformations that we discuss. Moreover it is also possible to carry out the transformation when Q is chosen in a different manner, i.e., without necessarily associating x_ν with the identity matrix; this is discussed in details in appendix B.

A general conformal transformation on R^{d+1} is then represented by a quaternionic Mobius transformation

$$Q'_\mu = Ix'_\mu - i\sum_{j \neq \mu} \sigma_j x'_j = (\tilde{a}_1 Q_\mu - i\tilde{a}_2 I).(i\tilde{a}_3 Q_\mu + \tilde{a}_4 I)^{-1} \qquad (3.8)$$

where $\tilde{a}_1, \tilde{a}_2, \tilde{a}_3, \tilde{a}_4$ are quaternions obeying

$$Det\left[\tilde{a}_1 \tilde{a}_3^{-1} \tilde{a}_4 \tilde{a}_3 - \tilde{a}_2 \tilde{a}_3\right] = 1 \qquad (3.9)$$

Two successive transformations lead to another Mobius transformation where the matrices a_i get multiplied by matrix multiplication [29]. Consider transforming Q'_μ by a further mobius transformation,

$$Q''_\mu = Ix''_\mu - i\sum_{j \neq \mu} \sigma_j x''_j = (\tilde{a}'_1 Q'_\mu - i\tilde{a}'_2 I).(i\tilde{a}'_3 Q'_\mu + \tilde{a}'_4 I)^{-1} \qquad (3.10)$$

Then

$$Q''_\mu = (\tilde{a}''_1 Q_\mu - i\tilde{a}''_2 I).(i\tilde{a}''_3 Q_\mu + \tilde{a}''_4 I)^{-1} \qquad (3.11)$$

where

$$\begin{aligned}
\tilde{a}''_1 = \tilde{a}'_1\tilde{a}_1 + \tilde{a}'_2\tilde{a}_3 \qquad & \tilde{a}''_2 = \tilde{a}'_1\tilde{a}_2 + \tilde{a}'_2\tilde{a}_4 \\
\tilde{a}''_3 = \tilde{a}'_3\tilde{a}_1 + \tilde{a}'_4\tilde{a}_3 \qquad & \tilde{a}''_4 = \tilde{a}'_3\tilde{a}_2 + \tilde{a}'_4\tilde{a}_4
\end{aligned} \qquad (3.12)$$

However, for the $\mathrm{SL}(2, R) \sim \mathrm{SU}(1,1)$ subgroup generated by D, K_μ, P_μ these parameters become real numbers provided one chooses the quaternion Q_μ as in (3.6), i.e. with x^μ being the coefficient of the identity matrix. The action of the SU(1,1) transformations is then obtained by representing the generators by Pauli matrices as in (2.3). The operator $\mathrm{U}(\Pi^\mu)$ in (3.1) is then represented by the 2×2 matrix,

$$\begin{aligned}
\mathrm{U}(\Pi^\mu) = e^{-w(-\sigma_z + i\beta\sigma_x)} &= \begin{pmatrix} \tilde{a}_1 & \tilde{a}_2 \\ \tilde{a}_3 & \tilde{a}_4 \end{pmatrix} \\
\tilde{a}_1 = \left(\cosh w\nu_0 + \nu_0^{-1}\sinh w\nu_0\right), &\quad \tilde{a}_4 = \left(\cosh w\nu_0 - \nu_0^{-1}\sinh w\nu_0\right) \\
\tilde{a}_2 = \tilde{a}_3 = -i\beta\nu_0^{-1}\sinh w\nu_0
\end{aligned} \qquad (3.13)$$

with $\tilde{a}_1\tilde{a}_4 - \tilde{a}_2\tilde{a}_3 = 1$. To find the transformed coordinates, we note that the quaternion matrix Q_μ transforms, upon action of $\mathrm{U}(\Pi^\mu)$ to Q'_μ given by [27–30]

$$\begin{aligned}
Q'_\mu = Ix'_\mu - i\sum_{j \neq \mu} \sigma_j x'_j &= (\tilde{a}_1 Q_\mu - i\tilde{a}_2 I).(i\tilde{a}_3 Q_\mu + \tilde{a}_4 I)^{-1} \\
&= \begin{pmatrix} \frac{x_\mu(2\tilde{a}_1\tilde{a}_4-1)-i(\tilde{a}_2\tilde{a}_4-\tilde{a}_1\tilde{a}_3 r^2)-ix_{\nu_1}}{\tilde{a}_4^2+2i\tilde{a}_3\tilde{a}_4 x_\mu-\tilde{a}_3^2 r^2} & \frac{-i(x_{\nu_2}-ix_{\nu_3})}{\tilde{a}_4^2+2i\tilde{a}_3\tilde{a}_4 x_\mu-\tilde{a}_3^2 r^2} \\ \frac{-i(x_{\nu_2}+ix_{\nu_3})}{\tilde{a}_4^2+2i\tilde{a}_3\tilde{a}_4 x_\mu-\tilde{a}_3^2 r^2} & \frac{x_\mu(2\tilde{a}_1\tilde{a}_4-1)-i(\tilde{a}_2\tilde{a}_4-\tilde{a}_1\tilde{a}_3 r^2)+ix_{\nu_1}}{\tilde{a}_4^2+2i\tilde{a}_3\tilde{a}_4 x_\mu-\tilde{a}_3^2 r^2} \end{pmatrix}
\end{aligned} \qquad (3.14)$$

where $\mu \neq \nu_1, \nu_2$, and ν_3. The transformed coordinates are then obtained from the relation $x'_\alpha = \mathrm{Tr}[\tau_\alpha^{-1} Q'_\mu]/2$ and yields

$$x'_\mu = \frac{x_\mu(2\tilde{a}_1\tilde{a}_4 - 1) - i(\tilde{a}_2\tilde{a}_4 - \tilde{a}_1\tilde{a}_3 r^2)}{\tilde{a}_4^2 + 2i\tilde{a}_3\tilde{a}_4 x_\mu - \tilde{a}_3^2 r^2}, \quad x'_\nu = \frac{x_\nu}{\tilde{a}_4^2 + 2i\tilde{a}_3\tilde{a}_4 x_\mu - \tilde{a}_3^2 r^2} \qquad (3.15)$$

Substituting eq. (3.13) in eq. (3.15), one recovers eqs. (3.4) and (3.5). This shows that the quaternionic approach provides a vastly simpler way to obtain the transformed coordinates.

In the rest of the paper we will deal with $d = 3$. The transformation from $R \times S^3$ to R^4 is given by

$$\tau = e^w \cos\theta, \, x = e^w \sin\theta\cos\phi, \, y = e^w \sin\theta\sin\phi\cos\psi, \, z = e^w \sin\theta\sin\phi\sin\psi, \qquad (3.16)$$

where $w_\mu = (w, \theta, \phi, \psi)$ are the coordinates on the cylinder $R \times S^3$, and w denotes time on the cylinder.

The above transformations are in euclidean signature. Upon continuation to real time $w \to \tilde{w} = -iw$ while the angles remain the same. Let us denote the analytically continued transformation matrix by

$$U = \begin{pmatrix} a & b \\ c & d \end{pmatrix} \qquad (3.17)$$

For the transformation (3.13) we have $a = d^\star$ while $b = c^\star = $ real. Using (3.15) it may be checked that the transformed time, $\tilde{w}'$ and the transformed angles θ', ϕ', ψ' remain real.

We will be interested in time evolution with square pulse protocol with different β and different Π_μ in different intervals. When these hamiltonians have the *same* Π_μ the time evolution in the different intervals correspond to transformations which lie in the *same* $SU(1,1)$ *subgroup* of the conformal group. In this case the net transformation can be simply obtained by usual matrix multiplication of the different U's. The net parameters will obey $a = d^\star$ and $b = c^\star$, which are the $SU(1,1)$ conditions, but b, c will not be in general real. However, the $SU(1,1)$ conditions are sufficient to ensure that the transformed coordinates on $(time) \times S^3$ are real.

The expression (3.13) shows that the behavior of the system under real time evolution depends on β. Continuing to real time $\tilde{w}$ and recalling that ν_0 is given by (3.2) and we see that the resulting conformal transformation involves trigonometric functions of time for $\beta < 1$, hyperbolic functions for $\beta > 1$ and power laws when $\beta = 1$. Thus for late times, observables will decay exponentially in time for $\beta > 1$ and oscillate when $\beta < 1$.

While we have illustrated this formalism for $d = 3$ the same formalism can be used for $d = 1, 2$ by setting some of the coordinates in eq. (3.7) to zero.

4 Floquet dynamics

In this section, we shall study Floquet dynamics of $3 + 1$ dimensional CFTs, using a square pulse protocol, described below. The protocols we consider have different hamiltonians in successive time intervals and we choose these time intervals to be equal. We will compute various physical properties at the end of each cycle. The strategy can be generalized to

arbitrary number of cycles. We defer the analysis for multiple cycles to future work. In what follows, we shall choose the amplitude of the pulses within a drive period (denoted by β below) to be same for simplicity.

In most of this section, we shall focus on dynamics of driven system at the end of a drive cycle; more specifically, we shall study the behavior of the operator expectation and fidelity starting from a primary state and unequal time correlators starting from vacuum, at $t = T$ as a function of T and β. Here T is the time extent (or time period) of a single cycle. Our analysis can be extended to study the micromotion (dynamics for $t \leq T$) of these quantities; however, in the present work we focus on their properties at $t = T$.

The corresponding macromotion, which yields information about stroboscopic dynamics of the driven system at $t = nT$ ($n \in Z$ and $n > 1$), is governed by the Floquet Hamiltonian H_F; we shall derive H_F for a class of drive protocols involving a single $SU(1,1)$ subgroup in section 4.4. In section E we discuss the structure of fixed points and surfaces for this special case. However, the corresponding analysis of macromotion for a generic drive protocol which involves multiple $SU(1,1)$ subgroups is more complicated and is left as a subject of future study.

The strategy will be to perform the computations on R^4 (coordinates x^μ), Weyl transforming to $R \times S^3$ (coordinates w^μ), and finally analytically continuing to real time $t = iw$. Under the Weyl transformation, a primary operator with conformal dimension Δ transforms as

$$O_\Delta(w_\mu) = e^{w\Delta} O_\Delta(x_\mu). \tag{4.1}$$

We shall use these relations to transform between the physical coordinates w_μ on the cylinder and those on the plane (x_μ).

As discussed above, unitary time evolution governed by a Hamiltonian of the form (1.1) is equivalent to a conformal transformation $x_\mu \to x'_\mu$ given by (3.15). The transformation of the primary operators of the CFT having conformal dimension Δ due to such dynamics is given by [31]:

$$O(x_\mu) \to U^\dagger O(x_\mu) U = O(x'_\mu) J_2^{\Delta/4}, \quad J_2 = \left| \frac{\partial x'_\mu}{\partial x_\nu} \right| = |\text{Det}[i\tilde{a}_3 Q + \tilde{a}_4 I]|^{-4} \tag{4.2}$$

where the last expression holds if the coordinates $\mathbf{x}'$ and $\mathbf{x}$ are related by the transformation given by eqs. (3.13) and (3.14).

4.1 Fidelity

In this section, we shall compute the fidelity $F(T)$ of a primary state $|\Delta\rangle$ of the CFT at the end of a drive cycle. This is defined, in Euclidean time, as

$$F(T_0) = \frac{\langle \Delta | U(T_0, 0) | \Delta \rangle}{\langle \Delta | \Delta \rangle} = \frac{\lim_{x_{2\mu} \to \infty, x_{1\mu} \to 0} \langle 0 | \phi(\mathbf{x}_2) U(T_0, 0) \phi(\mathbf{x}_1) | 0 \rangle}{\lim_{x_{2\mu} \to \infty, x_{1\mu} \to 0} \langle 0 | \phi(\mathbf{x}_2) \phi(\mathbf{x}_1) | 0 \rangle} \tag{4.3}$$

where $\phi(\mathbf{x}) \equiv \phi(\tau, x, y, z)$ denotes a primary CFT field of dimension h, $T = -iT_0$ is the drive period in real time and $|0\rangle$ denotes the CFT vacuum. Throughout this section, we shall work in Euclidean time and analytically continue to real time whenever necessary.
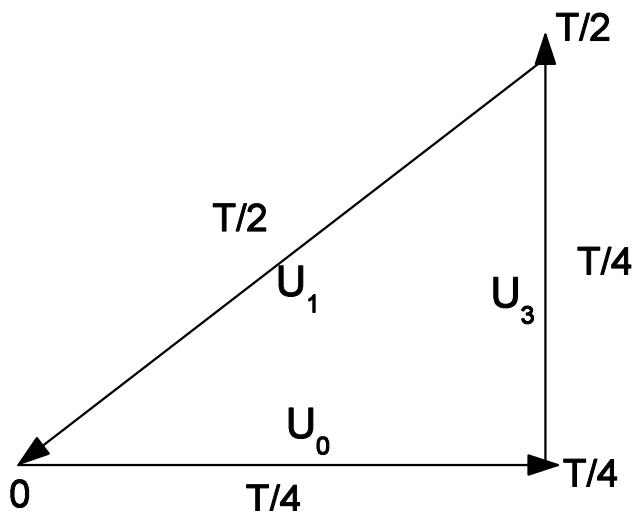
Figure 1. Schematic representation of the protocol for computing fidelity $F(t)$. See text for details.

The protocol we choose for computing $F(T)$ is schematically shown in figure 1. The evolution operator $\mathrm{U}(\Pi^\mu)$ in each cycle is chosen to be

$$\mathrm{U}(\Pi^\mu; \tau, 0) = e^{-H(\Pi^\mu)\tau}, \quad H(\Pi^\mu) = i(2D + \beta(K_\mu + P_\mu)\Pi^\mu \,. \tag{4.4}$$

The total evolution operator at the end of one cycle is given by

$$U = U^\dagger(\Pi^1; 0, T_0/2)\mathrm{U}(\Pi^3; T_0/2, T_0/4)\mathrm{U}(\Pi^0; T_0/4, 0) \,, \tag{4.5}$$

$$\Pi^1 = (0, 1, 0, 0) \,, \quad \Pi^3 = (0, 0, 0, 1) \,, \quad \Pi^0 = (1, 0, 0, 0) \,. \tag{4.6}$$

Note that we use the different deformed CFT Hamiltonians with same deformation parameter β to generate the evolution operator U. The fidelity is computed at the end of the cycle.

To obtain $F(T)$, we first note that the two point correlation function of a primary operator with dimension Δ can be written in the quaternion formalism as [29]

$$C_0 = \langle 0|\phi(\mathbf{x}_2)\phi(\mathbf{x}_1)|0\rangle = \frac{1}{(\mathrm{Det}[Q(\mathbf{x}_2) - Q(\mathbf{x}_1)])^\Delta} \tag{4.7}$$

In the above equation we have not specified a subscript for the quaternions since this particular result is independent of which $Q_{(\mu)}$ we use. For the unequal-time correlation function under a transformation by $U_\mu(T, 0)$, this leads to

$$\begin{aligned}
C_1 &= \langle 0|U_\mu^\dagger(T, 0)\Pi^\mu\phi(\mathbf{x}_2)U_\mu(T, 0)\Pi^\mu\phi(\mathbf{x}_1)|0\rangle \\
&= \frac{1}{\mathrm{Det}[Q'_\mu(\mathbf{x}'_2) - Q_\mu(\mathbf{x}_1)]^\Delta} \mathrm{Det}[(i\tilde{a}_3 Q_\mu(\mathbf{x}_2) + \tilde{a}_4 I)^{-1}]^\Delta \\
&= \frac{1}{\mathrm{Det}[(\tilde{a}_1 Q_\mu(\mathbf{x}_2) - i\tilde{a}_2 I) - Q_\mu(\mathbf{x}_1)(i\tilde{a}_3 Q_\mu(\mathbf{x}_2) + \tilde{a}_4 I)]^\Delta} \,.
\end{aligned} \tag{4.8}$$

Note that the second term in the denominator vanishes when $x_{1\mu} \to 0$. Further when $x_{2\mu} \to \infty$, we find $C_1 \to 1/\mathrm{Det}[\tilde{a}_1 Q_{\mu_1}(\mathbf{x}_2)]^\Delta$. Furthermore similar analysis shows for multiple
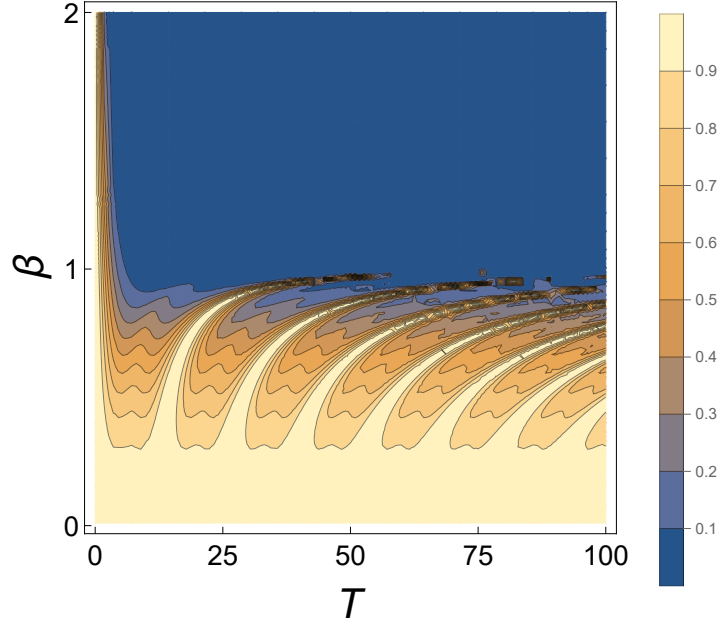
Figure 2. Plot of $|F(T)|$ as a function of β and T with $\Delta = 1$. For $\beta < 1$, $|F(T)|$ oscillates with T characterizing the non-heating phase and reaches $\simeq 1$ for $\nu = n\pi$ where n is an integer. For $\beta > 1$, $|F(T)|$ decays exponentially with T which is a signature of the heating phase.

subsequent transformations given by

$$U_{\mu_i}\Pi^\mu = \begin{pmatrix} \tilde{a}_i & \tilde{b}_i \\ \tilde{c}_i & \tilde{d}_i \end{pmatrix}, \quad \tilde{a}_i\tilde{d}_i - \tilde{b}_i\tilde{c}_i = 1 \tag{4.9}$$

$C_1 \to 1/\mathrm{Det}[(\prod_i \tilde{a}_i)Q_{\mu_i}(\mathbf{x}_2)]^\Delta$. This allows us to write the final expression for $F(T_0)$

$$F(T_0) = \frac{1}{(\tilde{a}_0(T_0)\tilde{a}_3(T_0)\tilde{a}_1(T_0))^\Delta} \tag{4.10}$$

To compute the $\tilde{a}_0$, $\tilde{a}_1$ and $\tilde{a}_3$, we use the 2×2 matrix representation of the operators D, K_μ and P_μ given in eq. (2.3). Using this one can write

$$U_\mu(\tau)\Pi^\mu = e^{-\tau\sqrt{1-\beta}^2(-n_z\sigma_z + n_x\sigma_x)}, \quad n_z = \frac{1}{\sqrt{1-\beta^2}}, \quad n_x = \frac{i\beta}{\sqrt{1-\beta^2}} \tag{4.11}$$

Defining $\nu = \sqrt{1-\beta^2}T/4$, we find, after analytically continuing to real time $T = -iT_0$ and using $\tilde{a}_\mu(T_0) = a_\mu(T)$

$$a_0(T) = a_3(T) = (\cos\nu + iT(4\nu)^{-1}\sin\nu), \quad a_1(T) = (\cos 2\nu - iT(2\nu)^{-1}\sin 2\nu)$$

$$F(T) = \frac{1}{[(\cos\nu + iT(4\nu)^{-1}\sin\nu)^2(\cos 2\nu - iT(2\nu)^{-1}\sin 2\nu)]^\Delta} \quad \text{for } \beta \neq 1$$

$$= \left(\frac{1}{(1 + iT/4)^2(1 - iT/2)}\right)^\Delta \quad \text{for } \beta = 1 \tag{4.12}$$

The behavior of each of the a_i and hence $F(T)$ depends crucially on the value of the parameter β. For $\beta < 1$ these are oscillatory functions of the time T, while for $\beta > 1$ they

decay exponentially for large T. These two behaviors are higher dimensional versions of the non-heating and heating phases. In between these phases there is a critical point $\beta = 1$ where we have a power law decay in time, $|F(T)| \sim 1/[(1 + T^2/16)^2(1 + T^2/4)]^{\Delta/2}$. This behavior is charted out in figure 2 which shows the behavior $|F(T)|$ for $\Delta = 1$. In between, at $\beta = 1$, we find a line which represents a critical line separating the two phases.

Our analysis of $F(T)$ indicates special frequencies at which $|F(T)| = 1$ indicating perfect overlap of the driven state with the initial states. These frequencies, which exist only in the non-heating phase can be read off from eq. (4.12) and are given by $T = T_n^*(\beta)$ where

$$T_n^*(\beta) = 4n\pi/\sqrt{1 - \beta^2}, \tag{4.13}$$

and n is an integer. The existence of these frequencies can also be seen in figure 2.

Thus we find that under a drive schematically represented by figure 1, F exhibits perfect revival at special frequencies in the non-heating phase and an exponential (power-law) decay with T in the heating phase (on the critical line).

The different behaviors for different values of β reflect the properties of the Hamiltonians used for time evolutions which have been discussed in the previous section. Each of these Hamiltonians represent a *different* SU(1, 1) subgroup of the conformal group. We chose the same β for each of the three Hamiltonians, so the conjugacy classes of each of these SU(1, 1) are the same. The results can be trivially extended to the cases where the three β's are different.

The above procedure can be also used to calculate transition amplitudes between a primary state and its descendants. In $1 + 1$ dimensions there are eficient algorithms to do this [32]: it will be interesting to see if an analogous proecure can be developed in higher dimensions.[3]

4.2 Unequal-time correlators

In this section, we compute the unequal-time two-point correlation function of the primary fields with conformal dimension Δ in the presence of a drive. We consider the fields on a cylinder and map them onto the plane using eq. (3.16). The initial coordinates on the plane corresponds to

$$\mathbf{x_2} = (\tau_2, x_2, y_2, z_2) = (\cos\theta_2, \sin\theta_2\cos\phi_2, \sin\theta_2\sin\phi_2\cos\psi_2, \sin\theta_2\sin\phi_2\sin\psi_2),$$
$$\mathbf{x_1} = (\tau_1, x_1, y_1, z_1) = (1, 0, 0, 0) \tag{4.14}$$

where we have taken initial time on the cylinder $w = 0$ without loss of generality. We have also chosen the coordinates $\theta_1 = 0$ for simplicity. In what follows we shall consider the correlation function

$$C_1(T) = \langle 0|U^\dagger(T, 0)O(\mathbf{x_2})U(T, 0)O(\mathbf{x_1})|0\rangle = \frac{J_2^{\Delta/4}}{(\text{Det}[Q(\mathbf{x_2'}) - Q(\mathbf{x_1})])^\Delta} \tag{4.15}$$

where $\mathbf{x_2'}$ represents the transformed coordinate and J_2 denotes the Jacobian of the coordinate transformation.

---

[3]We thank the referee for a question about this issue.
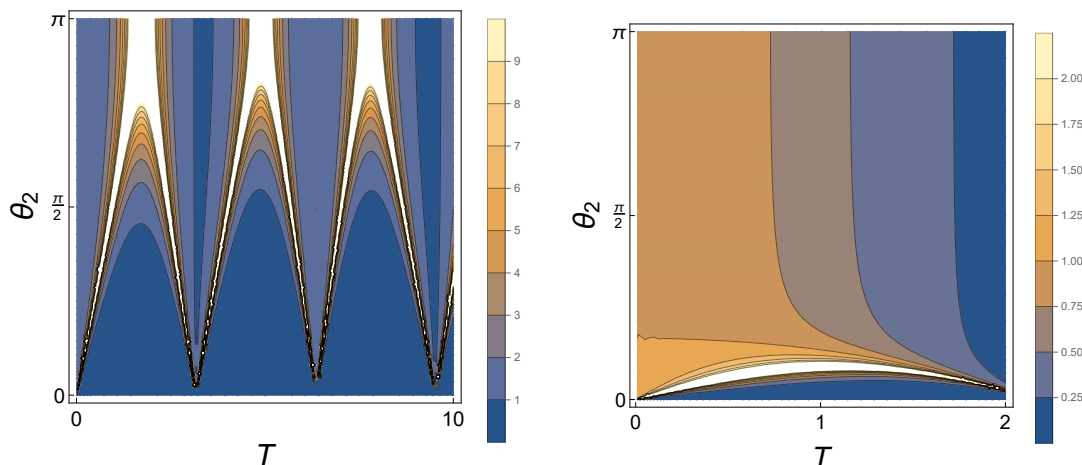
Figure 3. Plot of $|C_1(T)/C_1(0)|$ as a function of θ_2 and T for $\beta = 0.2$ (left panel) and $\beta_1 = 1.2$ (right panel) corresponding to a square pulse protocol. See text for details.

To study the dynamics, we first consider a square pulse protocol given by

$$
\begin{aligned}
H &= H_{(-)} = 2iD && \text{for } t \leq T/2 \\
H &= H_{(+)} = 2iD + i\beta\left(K_0 + P_0\right) && \text{for } t > T/2.
\end{aligned}
\tag{4.16}
$$

We will calculate the correlator at time T.

The evolution operator for this is

$$
\mathrm{U}(T,0) = U_0(T,0) = e^{-T_0(2iD + i\beta(K_0 + P_0))/2}e^{-iDT_0} = \begin{pmatrix} \tilde{a} & \tilde{b} \\ \tilde{c} & \tilde{d} \end{pmatrix}
$$

$$
a = d^* = \left(\cosh \eta T/2 + \frac{i}{\eta}\sinh \eta T/2\right)e^{iT/2}, \quad b = c^* = e^{-iT/2}\frac{\beta}{\eta}\sinh \eta T/2, \tag{4.17}
$$

$$
Q_0(\mathbf{x}_2') = (aQ_0(\mathbf{x}_2) - ibI).(icQ_0(\mathbf{x}_2) + dI)^{-1}, \; J_2 = |(\mathrm{Det}[icQ_0(\mathbf{x}_2) + dI])^{\Delta}|^{-4} \tag{4.18}
$$

where $\eta = \sqrt{\beta^2 - 1}$ and I is the 2×2 identity matrix. Here we have used eqs. (3.13) and (3.15), performed a Wick rotation $T = -iT_0$, and denoted $\tilde{a}(T_0)$, $\tilde{b}(T_0)$, $\tilde{c}(T_0)$, and $\tilde{d}(T_0)$ after the rotation as $a(T)$, $b(T)$, $c(T)$, and $d(T)$ respectively. Substituting eqs. (4.18) in eq. (4.15), we find after transforming back to cylinder coordinates[4]

$$
C_1(T) = C_1(0)\left[\frac{2(1 - \cos\theta_2)}{(a - ic)^2 - (b - id)^2 - 2i(a - ic)(b - id)\cos\theta_2}\right]^{\Delta},
$$

$$
C_1(0) = \frac{1}{2(1 - \cos\theta_2)^{\Delta}} \tag{4.19}
$$

The dependence of $C_1(T)$ on both T and β can be obtained by substituting the expressions of a, b, c and d from eq. (4.18). We note that for $\beta > 1$, the system is in the heating phase and the correlation decays exponentially; in contrast, for $\beta < 1$, the dynamics is oscillatory. Also, we find that $C(T)$ depends only on θ_2 and is independent of other coordinates. This

---

[4]The Weyl factors cancel in the following expressions.

is a consequence of the choice of the drive protocol which involves only K_0 and P_0. These features of the correlation function are shown in figure 3 where $|C_1(T)/C_1(0)|$ is plotted for $\Delta = 1$ as a function of θ_2 and T for $\beta = 0.2$ (left panel) and $\beta = 1.2$ (right panel).

We next consider a drive protocol involving two different sets of generators given by

$$H_{(-)} = 2iD + i\beta(K_{(0)} + P_{(0)}), \qquad\qquad H_{(+)} = 2iD + i\beta(K_{(3)} + P_{(3)})$$

$$\mathrm{U}(T_0, 0) = U_{(+)}(T_0, T_0/2)U_{(-)}(T_0/2, 0), \qquad U_{(\pm)}(\tau, 0) = e^{-\tau H_{(\pm)}/\hbar} = \begin{pmatrix} \tilde{a}_\pm & \tilde{b}_\pm \\ \tilde{c}_\pm & \tilde{d}_\pm \end{pmatrix} \qquad (4.20)$$

To obtain the correlator corresponding to this protocol, we consider the action of U_- on $Q(\mathbf{x}_2) \equiv Q_2$ which is given by

$$Q_2^{(1)} = (\tilde{a}_- Q_2 - i\tilde{b}_- I).(i\tilde{c}_- Q_2 + \tilde{d}_- I)^{-1} = \begin{pmatrix} \tau' - iz' & -i(x' - iy') \\ -i(x' + iy') & \tau' + iz' \end{pmatrix}$$

$$\tau' = \frac{\tau(2\tilde{a}_- \tilde{d}_- - 1) - i(\tilde{a}_- \tilde{c}_- - \tilde{b}_- \tilde{d}_- r^2)}{\tilde{d}_-^2 + 2i\tilde{c}_- \tilde{d}_- \tau - \tilde{c}_-^2 r^2}, \qquad x'_j = \frac{x_j}{\tilde{d}_-^2 + 2i\tilde{c}_- \tilde{d}_- \tau - \tilde{c}_-^2 r^2} \qquad (4.21)$$

where $x_j = (x, y, z)$ for $j = (1, 2, 3)$. Next, we rewrite $Q_2^{(1)}$ as $Q_2^{'(1)} = z'I - i\sigma_z \tau' - i\sigma_x x' - i\sigma_y y'$ and perform the second transformation

$$Q_2^{(2)} = (\tilde{a}_+ Q_2^{'(1)} - i\tilde{b}_+ I).(i\tilde{c}_+ Q_2^{'(1)} + \tilde{d}_+ I)^{-1} = \begin{pmatrix} z'' - i\tau'' & -i(x'' - iy'') \\ -i(x'' + iy'') & z'' + i\tau'' \end{pmatrix}$$

$$z'' = \frac{z'(2\tilde{a}_+ \tilde{d}_+ - 1) - i(\tilde{a}_+ \tilde{c}_+ - \tilde{b}_+ \tilde{d}_+ r'^2)}{\tilde{d}_+^2 + 2i\tilde{c}_+ \tilde{d}_+ z' - \tilde{c}_+^2 r'^2}, \qquad x''_j = \frac{x'_j}{\tilde{d}_+^2 + 2i\tilde{c}_+ \tilde{d}_+ z' - \tilde{c}_+^2 r'^2} \qquad (4.22)$$

where $x''_j = (\tau'', x'', y'')$ for $j = (1, 2, 3)$.

The rest of the calculation is cumbersome but straightforward. A somewhat lengthy algebra yields

$$C_2(T) = C_1(0) \left(\frac{2(1 - \cos\theta_2)}{\alpha + \beta_1 \cos\theta_2 + \beta_2 \sin\theta_2 + \beta_3 \cos 2\theta_2 + \gamma(\theta_2)\sin\theta_2 \sin\phi_2 \sin\psi_2} \right)^\Delta . \qquad (4.23)$$

Here α, β_i ($i = 1, 2, 3$), and γ are functions of the drive parameters through functions a, b, c and d given by

$$a = d^* = \left(\cosh \eta T/2 + \frac{i}{\eta} \sinh \eta T/2 \right), \quad b = c = \frac{\beta}{\eta} \sinh \eta T/2, \qquad (4.24)$$

$$\gamma(\theta_2) = -4ib(a - d)(b^2 - d^2 - 2ibd\cos\theta_2), \quad \beta_2 = b^2 - a^2$$

$$\beta_3 = \frac{1}{2}\Big[8a^3 d(1 - ad) + a^2(-1 + 8(b + 2id)d^2) - 8iabd(d + b(2bd - i))$$

$$+ b^2(1 + 8d(ib - d(b^2 - d^2))) \Big]$$

$$\beta_1 = 4i\Big[2a^4 bd - c^3 b(1 + 2d^2) + a(b^3 + ib^2 d(1 + 4b^2) + 2b^3 d^2 - id^3) - b^3 d(1 + 4d^2)$$

$$+ a^2 d(b - 2b^3 - 4ib^2 c4 + 2id^3) + b(2b^4 d + ibd^2 + 2d^5 - ib^3(1 + 2d^2)) \Big]$$

where we have analytically continued to real time $T = -iT_0$. The function α is cumbersome but can be expressed in terms of a, b, c and d.
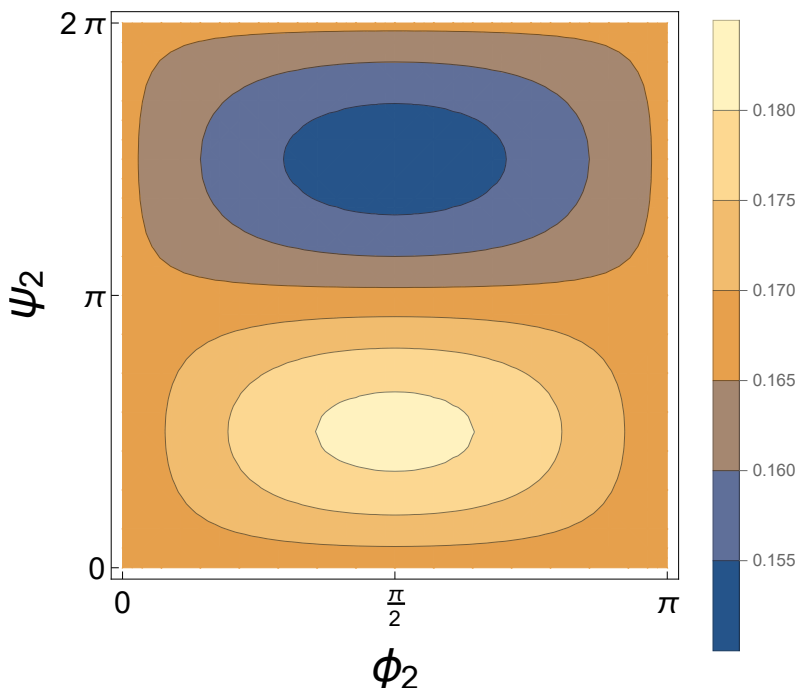
Figure 4. Plot of $|C_2(T)/C_2(0)|$ as a function of ϕ_2 and ψ_2 for $\beta = 0.2$, $T = 5$ and $\theta = \pi/4$. See text for details.

Eq. (4.23) indicates a clear rotational symmetry breaking in the correlation function. This is a consequence of application of two different sets of generators (K_0, P_0) and (K_3, P_3) for constructing $U(T, 0)$. This dependence is shown for a fixed $T = 1$, $\theta_2 = \pi/4$ and $\beta = 0.2$ in figure 4 where $|C_2(T)/C_2(0)|$ is plotted as a function of ϕ_2 and ψ_2.

4.3 Local probes of the driven state

In this section we will probe the time-evolving state with local operators, i.e., we are interested in computing:

$$\langle \Delta | U_\mu^\dagger(T, 0) \Pi^\mu A(w^\alpha) U_\mu(T, 0) \Pi^\mu | \Delta \rangle. \tag{4.25}$$

We will find here as in the $d = 1$ case [33] that there is localization in the local observables.

Energy density

Consider first the energy density, i.e. when the operator $A(w^\alpha)$ is chosen to be $T_{ww}(w^\alpha)$. Therefore we will need the transformation of the stress tensor. For $d = 3$, the conformal dimension of the energy-momentum tensor is 4, so that the Weyl factor is simply e^{4w}. Along with the factors coming from the transformation of a spin-2 tensor, the energy density translates to

$$T_{ww}(w^\mu) = e^{4w} \frac{\partial x^\rho}{\partial w} \frac{\partial x^\sigma}{\partial w} T_{\rho\sigma}(x) + \frac{3a}{8\pi^2}, \tag{4.26}$$

where the last term comes from the Weyl anomaly. Conjugation of the R^{d+1} stress tensor $T_{\rho\sigma}(x)$ gets with the deformed evolution operators $U_\mu(T,0)\Pi^\mu$ leads to a conformal transformation. In D flat spacetime for a spin-2 conformal primary like the stress-tensor the transformation rule is:

$$U^\dagger T_{\mu\nu}(x)U = T'_{\mu\nu}(x) = J^{\frac{D-2}{D}} \frac{\partial x'^\rho}{\partial x^\mu} \frac{\partial x'^\sigma}{\partial x^\nu} T_{\rho\sigma}(x'),\tag{4.27}$$

where J denotes the Jacobian of the conformal transformation. Finally we shall be left to compute a plane three point function involving a stress-tensor and two primaries. This is given by [34]:

$$\langle O(x_1)O(x_2)T^{\mu\nu}(x_3)\rangle = -\frac{4\Delta}{6\pi^2} \frac{H^{\mu\nu}(x_1,x_2,x_3)}{|x_{12}|^{2\Delta-2}|x_{13}|^2|x_{23}|^2},\tag{4.28}$$

$$\text{where, } H^{\mu\nu} = V^\mu V^\nu - \frac{1}{4}V^2\delta^{\mu\nu}, \text{ with, } V^\mu = \frac{x_{13}^\mu}{x_{13}^2} - \frac{x_{23}^\mu}{x_{23}^2}.$$

Putting everything together, the time-dependent piece (i.e. modulo the anomalous piece) in the energy density of the driven state is:

$$\langle\Delta|U^\dagger T_{ww}(w^\mu)U|\Delta\rangle_T = -2\frac{\Delta}{3\pi^2} \frac{e^{4w}J_2^{-1/2}}{|x'(w^\mu)|^2} \frac{\partial x^\rho}{\partial w} \frac{\partial x^\sigma}{\partial w} \frac{\partial x'^\alpha}{\partial x^\rho} \frac{\partial x'^\beta}{\partial x^\sigma} H_{\alpha\beta}(x'(w^\mu)),\tag{4.29}$$

$$\text{where, } H_{\rho\sigma}(x') = \frac{x'_\rho x'_\sigma - \frac{x'^2}{4}\delta_{\rho\sigma}}{(x')^4}.$$

We consider a square pulse drive given by:

$$H = H_{(-)} = 2iD \qquad \text{for } t \le T/2$$
$$H = H_{(+)} = 2iD + i\beta\left(K_{(1)} + P_{(1)}\right) \qquad \text{for } t > T/2.\tag{4.30}$$

For this protocol the evolution operator is parametrized as: $\begin{pmatrix} a & b \\ c & d \end{pmatrix}$ with a, b, c, d as in eq. (4.17). Below in figure 5 and figure 6 we plot the absolute value of the normalized energy density

$$E(\theta,\phi,\psi,T) = \frac{\langle\Delta|U^\dagger T_{ww}(w^\mu)U|\Delta\rangle_T}{\langle\Delta|U^\dagger T_{ww}(w^\mu)U|\Delta\rangle_{T=0}}\tag{4.31}$$

in various regimes. Note that β denotes the amplitude of the deformation and can be used to enter and leave the heating regime. When $\beta > 1$ and we are in the heating regime we find clear signatures of localization of the energy density in the angular directions, whereas the non-heating regime is characterized by oscillations. Furthermore the localization occurs in both the angular directions θ and ϕ as is clear from the density plot of figure 7, and is independent of the ψ direction. Due to the latter feature we omit ψ from $E(\theta,\phi,\psi,T)$.

The explicit formula for the energy density as obtained from the analytic expression eq. (4.29) turns out to be too complicated. Thus we turn our attention to a simpler observable, namely, that of a local primary probe in the driven state, which allows for an explanation of the angular localization.
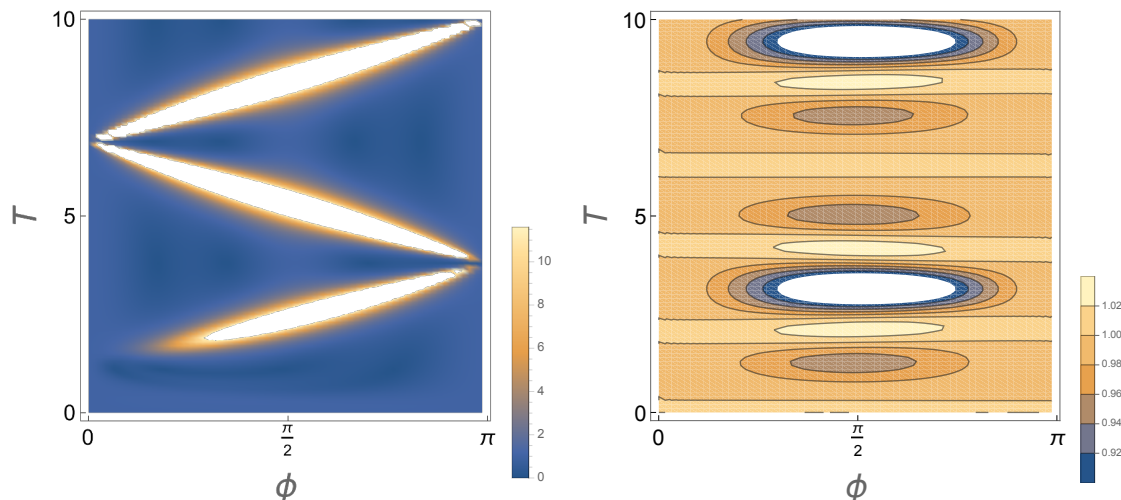
Figure 5. Density plots of normalized density $|E(\theta, \phi, T)|$ in the ϕ, T plane for $\theta = \pi/2$. Left Panel: in the heating phase with $\beta = 1.2$ we find progressive localization. Right panel: in the non-heating phase with $\beta = 0.09$ we find oscillations.
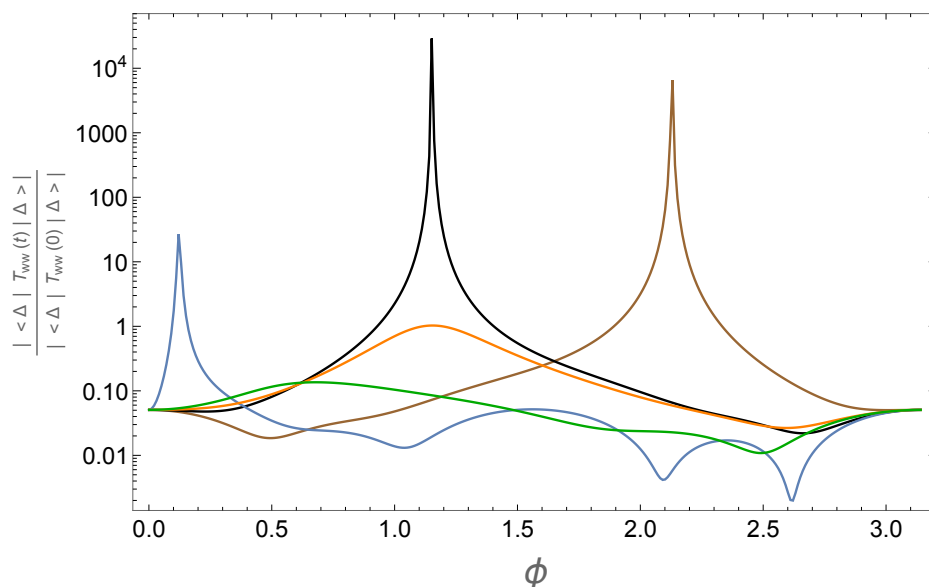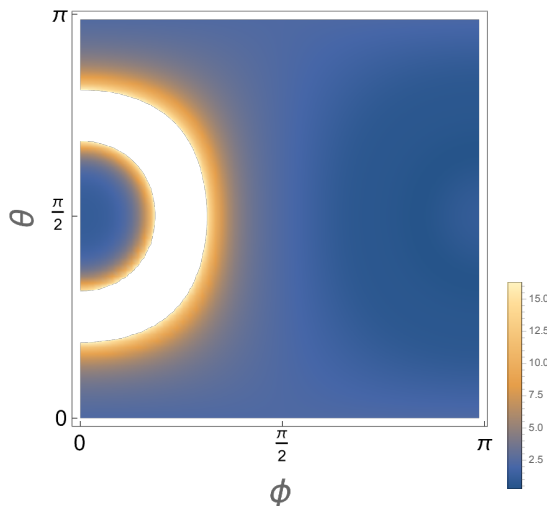

Figure 6. Plots of normalized density $|E(\theta, \phi, T)|$ as a function of ϕ for $\theta = \pi/2$ in the heating phase, $\beta = 1.2$, and for several representative values of T: 1.5 (Green), 2 (Orange), 7 (Blue), 9 (Brown) and 12 (Black).

Primaries

Here we choose the probe to be another primary operator in place of $A(w^\alpha)$ in eq. (4.25). The transformation rule of a primary is already given as in eq. (4.2), using which along with the Weyl factor, eq. (4.1), and the universal formula for three point primary correlator, we obtain:

$$\langle \Delta | U_\mu^\dagger \Pi^\mu(T, 0) O_{\Delta_1}(w^\alpha) U_\mu(T, 0) \Pi^\mu | \Delta \rangle = e^{w\Delta_1} J_2^{\Delta_1/4} \frac{C_{\Delta\Delta\Delta_1}}{|x'|^{\Delta_1}}, \qquad (4.32)$$

Figure 7. Density plots of normalized density $|E(\theta, \phi, T)|$ in the ϕ, θ plane for $T = 6$, in the heating phase, $\beta = 1.1$.

where $C_{\Delta\Delta_1}$ is the operator product expansion coefficient which is part of the CFT data. The above expression in the cylindrical coordinates, with initial time $w = 0$, for a generic $SU(1,1)$ drive in the x direction, takes the form:

$$\langle \Delta | O_{\Delta_1}(T) | \Delta \rangle = C_{\Delta\Delta_1} \frac{[((1 + a_2 a_3)^2 - a_2^2 a_4^2)^2 + 4a_2^2 a_4^2(1 + a_2 a_3)^2 \cos^2\phi \sin^2\theta]^{-\Delta_1/4}}{a_4^{-4\Delta_1}[a_4^4(a_3^2 - a_4^2)^2 + 4a_3^2 a_4^6 \sin^2\theta \cos^2\phi]^{3\Delta_1/4}}$$

$$= C_{\Delta\Delta_1} O(\theta, \phi, T)_\Delta. \tag{4.33}$$

Once again there is independence in ψ. Notice that when either $\theta = 0$ or $\phi = \pi/2$ the above becomes space independent. Once again, we consider the square-pulse protocol involving deformation in the x direction, as in eq. (4.30). The parameter β denotes the amplitude of the drive and can be used to enter and leave the heating regime. In figure 8 on the β, T plane we obtain a density plot very similar to figure 2. In particular we notice, that oscillations die into exponential fall-offs as the $\beta = 1$ line is crossed from below. At $\beta = 1$ the functional dependence of the absolute value squared of the one point function in the driven state is:
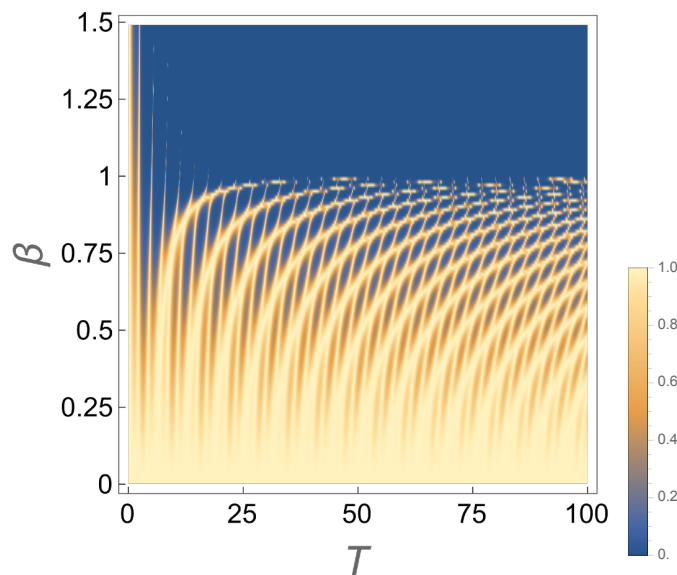
$$|O(\theta, \phi, T)|_\Delta^2 =$$
$$\Big((8 + 4T^2 + T^4 + T^2(T^2 - 4)\cos 2T + 4T^3 \sin 2T)^2 - 4T^2 \cos^2\phi (T^2(4 + T^2)^2$$
$$+ (8 + 4T^2 + T^4)((T^2 - 4)\cos 2T + 4T \sin 2T))\sin^2\theta + 4T^4(4 + T^2)^2 \cos^4\phi \sin^4\theta \Big)^{-\Delta_1}. \tag{4.34}$$

At large T, dropping the rapidly oscillatory pieces, we find:

$$|O(\theta, \phi, T)|_\Delta^2 \sim \frac{1}{T^{8\Delta_1}(1 - 2\cos^2\phi \sin^2\theta)^{2\Delta_1}} + \mathcal{O}(T^{-10\Delta_1}). \tag{4.35}$$

It turns out that the higher order terms in the $1/T$ series (with rapidly oscillating terms dropped) contains higher order singularities of $1 - 2\cos^2\phi \sin^2\theta$:

$$|O(\theta, \phi, T)|_\Delta^2 = \sum_{n=1}^\infty \frac{f_{n,\Delta_1}(\cos^2\phi \sin^2\theta)}{T^{\Delta_1(6+2n)}(1 - 2\cos^2\phi \sin^2\theta)^{\frac{1}{2}(2n+1-(-1)^n)\Delta_1}}. \tag{4.36}$$

Figure 8. Plot of $|O(\theta = 0, \phi, T)|_\Delta$ as a function of β and T with $\Delta_1 = 1$. For $\beta < 1$, we find oscillations with T characterizing the non-heating phase and for $\beta > 1$, the one-point function decays exponentially with T which is a signature of the heating phase.
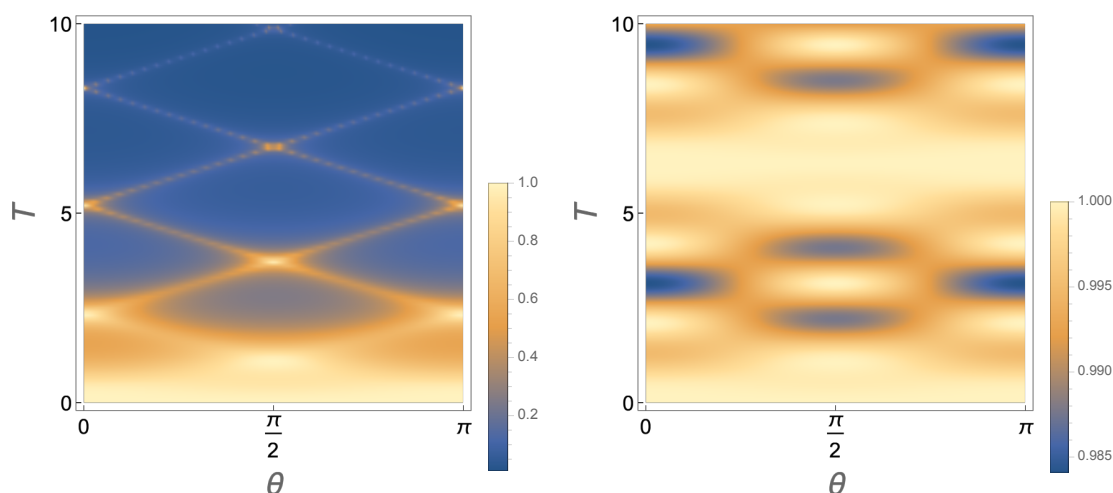
Figure 9. Density plots of normalized $|O(\theta, \phi, T)|_\Delta$ in the θ, T plane for $\phi = 0$. Left Panel: in the heating phase with $\beta = 1.1$ we find progressive localization. Right panel: in the non-heating phase with $\beta = 0.1$ we find oscillations. The conformal dimension is taken to be $\Delta_1 = 0.4$.

These singularities give rise to localization in the angular directions, and as we numerically investigate next, also persists in the heating, $\beta > 1$ regime.

Below in figure 9 we plot the normalized one point function amplitude in various regimes. We find clear signatures of localization of the amplitude in the angular directions, where as the non-heating regime is characterized by oscillations. Localization occurs in both the ϕ as well as θ directions as is clear from the left panel of figure 10. In the right panel of figure 10 we have plotted the contours of the function $\cos^2 \phi \sin^2 \theta$ since at least in the $\beta = 1$
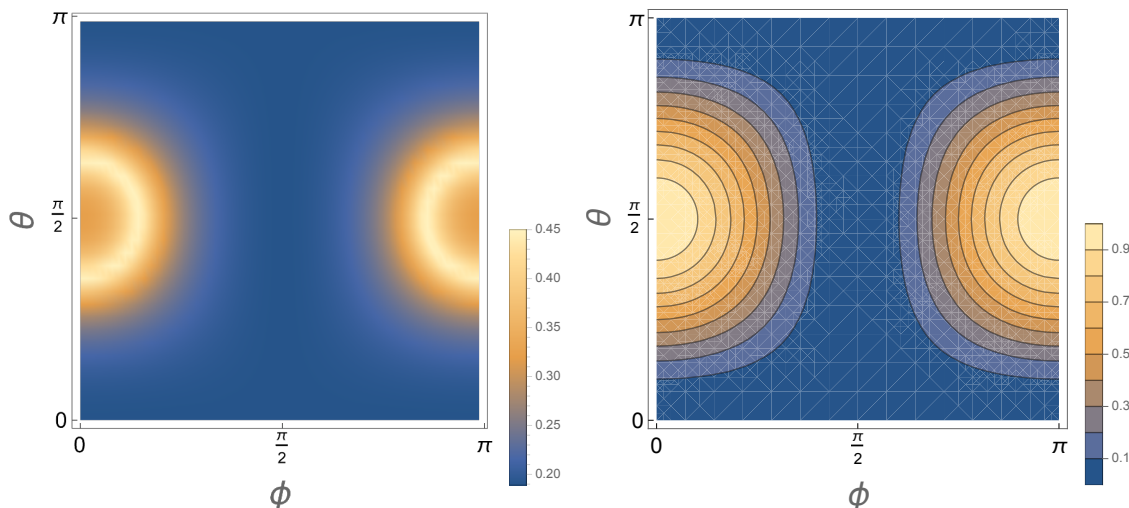
Figure 10. Left Panel: localization from the density plots of normalized $|O(\theta, \phi, T)|_\Delta$ in the ϕ, θ plane for $T = 3.3$, in the heating phase, $\beta = 1.1$. The conformal dimension is set to $\Delta_1 = 0.4$. Right Panel: contour lines of $\cos^2 \phi \sin^2 \theta$. See text for details.

line we expect from eq. (4.36) localization along the $\frac{1}{2}$ contour. The plots are indicative of the fact that similar singularities extend into the heating regime as well. It is very natural that a similar effect is responsible for the localization in the energy density when the primary gets replaced by the stress-tensor.

4.4 Floquet Hamiltonian for protocols involving a single SU(1,1) subalgebra and Dynamical Phases

In this sub-section, we shall derive the Floquet Hamiltonian for any periodic drive where the hamiltonians for each piece of a square pulse protocol all belong to the same SU(1,1) subgroup of the conformal group generated by D, K_μ, P_μ. As explained earlier the real time evolution over a single cycle of time extent T the evolution operator can be represented by a SU(1,1) matrix

$$\mathrm{U}(T,0) = \begin{pmatrix} a & b \\ b^* & a^* \end{pmatrix}$$

$$|a|^2 - |b|^2 = 1 \tag{4.37}$$

The parameters then determine the transformation of the quaternion as in (3.8),

$$Q'_\mu = (aQ_\mu - ibI)(ib^\star Q_\mu + a^\star I)^{-1} \tag{4.38}$$

The Floquet Hamiltonian $H_F(T)$ is defined by (in $\hbar = 1$ units)

$$\mathrm{U}(T,0) = \exp[-iH_F(T)T]. \tag{4.39}$$

This should be a linear combination of the generators

$$H_F(T) = i\alpha_1 D + i\alpha_2(K_\mu + P_\mu) + \alpha_3(K_\mu - P_\mu) \tag{4.40}$$

Here $\alpha_1, \alpha_2, \alpha_3$ are real numbers. This is ensured by the hermiticity properties of the hermitian hamiltonians in each portion of the square pulse protocol. For s given protocol $H_F(T)$ can be obtained by using a Baker-Hausdorff-Campbell rule. However, since the result depends only on the algebra one can instead use the representation (2.3) of the generators in terms of Pauli matrices σ_i. In this representation

$$H_F(T) \sim \sum_{i=x,y,z} \sigma_i \gamma_i \tag{4.41}$$

Note that it follows from the representation (2.3) that one must have γ_1, γ_2 purely imaginary and γ_3 real. Comparing eqs. (4.37) and (4.39) we can proceed to solve for γ_i.

There are three classes, corresponding to the three conjugacy classes of the SU(1,1) transformation. In the following we will denote

$$a_r = \text{Re}[a], \qquad a_I = \text{Im}[a], \qquad b_r = \text{Re}[b], \qquad b_I = \text{Im}[b] \tag{4.42}$$

1. $a_r^2 < 1$. This corresponds to $\sum_i \gamma_i^2 > 0$. In this case the transformation belongs to the elliptic conjugacy class. Then the Floquet hamiltonian is

$$H_F = \frac{\Lambda(T)}{\sqrt{1-a_r^2}} \left[2ia_I D + ib_r(K_\mu + P_\mu) - b_I(P_\mu - K_\mu) \right] \tag{4.43}$$

where

$$T\Lambda_e(T) = \arccos(a_r) \tag{4.44}$$

The evolution operator after n-cycles of the drive can be written as $\text{U}(nT,0) = \exp[-inH_F(T)T]$. In matrix form this can be written, for any integer n, as

$$\text{U}(nT,0) = \begin{pmatrix} a_n & b_n \\ b_n^* & a_n^* \end{pmatrix}$$
$$a_n = \cos(n\Lambda_e T) + i\frac{a_I}{\sin(\Lambda_e T)}\sin(n\Lambda_e T)$$
$$b_n = \frac{b_r + ib_I}{\sin(\Lambda_e T)}\sin n\Lambda_e T \tag{4.45}$$

These coefficients are periodic in the number of cycles n with a period T_p

$$T_p = \frac{2\pi}{\arccos(a_r)} \tag{4.46}$$

so that the stroboscopic time evolution is periodic. The system is in a non-heating oscillatory phase.

2. $a_r^2 = 1$. We now have $\sum_i \gamma_i^2 = 0$ and the transformation is in the parabolic conjugacy class. In this case one has

$$H_F = 2ia_I D + ib_r(K_\mu + P_\mu) - b_I(P_\mu - K_\mu) \tag{4.47}$$

At the end of n cycles we have

$$U(nT, 0) = \begin{pmatrix} a_n & b_n \\ b_n^* & a_n^* \end{pmatrix}$$

$$a_n = 1 + ina_I$$

$$b_n = n(b_r + ib_I) \tag{4.48}$$

As a function of n these grow linearly in n, leading to a response which grows with Floquet time in a linear fashion.

3. $a_r^2 > 1$. In this case one has $\sum_i \gamma_i^2 < 0$ and the transformation is the hyperbolic conjugacy class. Now the Floquet hamiltonian is

$$H_F = \frac{\Lambda_h(T)}{\sqrt{a_r^2 - 1}} \left[2ia_I D + ib_r(K_\mu + P_\mu) - b_I(P_\mu - K_\mu) \right] \tag{4.49}$$

where

$$T\Lambda_h(T) = \text{arccosh}(a_r) \tag{4.50}$$

The matrix which corresponds to time evolution by n cycles is now given by

$$U(nT, 0) = \begin{pmatrix} a_n & b_n \\ b_n^* & a_n^* \end{pmatrix}$$

$$a_n = \cosh n\Lambda_h T + i\frac{a_I}{\sinh(\Lambda_h T)} \sinh n\Lambda_h T$$

$$b_n = \frac{b_r + ib_I}{\sinh(\Lambda_h T)} \sinh n\Lambda_h T \tag{4.51}$$

For large stroboscopic times n the response of the system now grow exponentially in the Floquet time n, characteristic of a heating phase.

Since the phase in Floquet dynamics is determined by the conjugacy class of the corresponding conformal transformation it is possible to go between these phases by changing the time extents during which the different hamiltonians act within a single period. Consider for example a slight variation of the protocol (4.16),
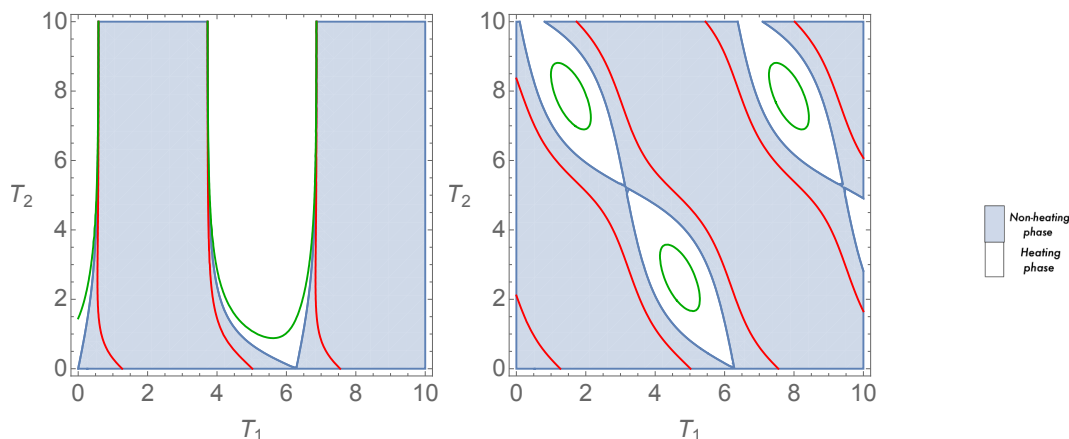
$$H = H_{(-)} = 2iD \qquad \text{for} \ \ t \leq T_1$$

$$H = H_{(+)} = 2iD + i\beta \left(K_0 + P_0 \right) \qquad \text{for} \ \ T_1 \leq t \leq T_1 + T_2. \tag{4.52}$$

The period is now $T = T_1 + T_2$. The corresponding matrix elements of (4.37) are given by, for $\beta > 1$,

$$a = e^{iT_1} \left(\cosh \eta T_2 + \frac{i}{\eta} \sinh \eta T_2 \right) \qquad b = e^{-iT_1} \frac{\beta}{\eta} \sinh \eta T_2, \quad \eta = \sqrt{\beta^2 - 1} \tag{4.53}$$

while for $\beta < 1$ we have

$$a = e^{iT_1} \left(\cos \nu T_2 + \frac{i}{\nu} \sin \nu T_2 \right) \qquad b = e^{-iT_1} \frac{\beta}{\nu} \sin \nu T_2, \quad \nu = \sqrt{1 - \beta^2} \tag{4.54}$$

Figure 11. Contours of $(\mathrm{Re}[a])^2$. Left Panel: we use equation (4.53) with $\beta = 1.2$. The blue line is $(\mathrm{Re}[a])^2 = 1$, the red line is $(\mathrm{Re}[a])^2 = 0.3$ for and the green line has $(\mathrm{Re}[a])^2 = 1.5$. Right panel: we use equation (4.54) with $\beta = 0.8$. The blue line is $(\mathrm{Re}[a])^2 = 1$, the red line is for $(\mathrm{Re}[a])^2 = 0.3$ and the green line has $(\mathrm{Re}[a])^2 = 1.5$.

The conjugacy class is determined by the real part of a, one can have heating as well as a non-heating phases in Floquet dynamics for any value of β. Left panel of figure 11 shows a contour plot of $(\mathrm{Re}[a])^2$ for $\beta = 1.2$, while right panel of figure 11 shows a contour plot of $\mathrm{Re}[a]$ for $\beta = 0.8$.

These figures show how that can get dynamical phase transitions between heating and non-heating phases by changing T_1 and T_2 both for $\beta < 1$ and for $\beta > 1$.

Finally, the different dynamical phases can be also understood in terms of the structure of fixed points of the quaternionic Mobius transformations (restricted to a single $\mathrm{SU}(1,1)$. This is discussed in appendix E.

Note that we are using the word "heating" in a heuristically — in the sense that the Floquet dynamics is exponentially damped as a function of the number of cycles. Thermalization in conformal field theories are non-standard. In $1 + 1$ dimensions the presence of an infinite number of KdV charges implies that the system can evolve into a Generalized Gibbs Ensemble (see e.g. [38]). We are not aware of an analogous result in higher dimensions.[5]

4.5 Floquet dynamics for protocols with different $\mathrm{SU}(1,1)$ subgroups

The preceding results for Floquet dynamics were for the special case where the protocol is such that the transformation belongs to a single $\mathrm{SU}(1,1)$ subgroup of the conformal group. When the protocol involves different $\mathrm{SU}(1,1)$ subgroups in different time intervals, as in the calculation of fidelity above, the entries in the net quaternionic Mobius transformation (3.8 cannot be chosen to be complex numbers with any choice of the quaternion representation. Consider for example a two step square pulse protocol where we first use a hamitonian $H(\Pi^0)$ for $0 < t < T/2$ and a hamiltonian $H(\Pi^1)$ for $T/2 < t < T$. In our calculations we dealt with this by switching the representation of quaternions, using Q_0 for the first interval and then collecting the transformed coordinates into a quaternion Q_1. However,

---

[5]We thank the referee for a comment about this point.

as explained in appendix B, we could have also used the quaternion representation Q_1 in the first step. This would lead to a transformed Q_1' given by (3.8) where the entries are themselves quaternions. In the next time interval the transformation on Q_1' is simple since the entries are now numbers. More generally, the net result for composing two different quaternionic transformations take the form (3.12).

A derivation of the Floquet hamiltonian is likewise more involved. We leave this important aspect to a future publication.

5 Discussions

In this paper we initiated a program of studying periodic quantum dynamics of driven deformed conformal field theories in arbitrary number of dimensions, inspired by recent work in $1+1$ dimensions. More concretely, we studied the properties of driven $3+1$ dimensional CFTs using square protocols which involve evolution by non-commuting Hamiltonians in successive time intervals after a single drive cycle.

There are several points worth emphasizing regarding this approach. First, the method of exactly computing the dynamics works in arbitrary number of dimensions. We performed explicit calculations in $3+1$ dimensions in this work. But our use of quaternion formalism provides a simple way to perform these calculations all $d \leq 3$. Secondly, our method can be straightforwardly generalized to other drive protocols including continuous ones; we leave this as a subject of future work. For a class of drive protocols which uses same μ but different β for each pulse within a drive cycle, we have shown how to obtain the necessary transformations for arbitrary number of cycles. This is similar to $d = 1$, and we can have dynamic control over the transition from the heating to the non-heating phase similar to that found in $d = 1$ driven CFTs [12, 14, 16]. Explicit results for multiple cycles of this type will appear in a future paper. For pulses with different μ, the situation is less clear and this issue is left as a subject of future study.

While the power of conformal symmetry allows us to calculate observables and the details associated with the phase structure, perhaps it is useful to ponder over a simpler physical intuition of the underlying physics. In this regard, it is useful to consider e.g. free theories in $(1 + 1)$-dimensions. For free Bosons, the stress-tensor $T(w) = (-1/2) : \partial\phi(w)\partial\phi(w) :$ and for free Fermions it is given by $T(w) = (1/2) : \psi(w)\partial\psi(w) :$ and subsequently the Virasoro modes are extracted from the stress-tensor: $L_n = (1/(2\pi i)) \oint w^{n+1} dw T(w)$. The standard radial quantization in CFT chooses a Hamiltonian $H \sim L_0$, which corresponds to a stress-tensors of the form: $\partial\phi(w)\partial\phi(w)$ for Bosons and $\psi(w)\partial\psi(w)$ for Fermions. Choosing a different Hamiltonian involving $\{L_m, L_{-m}\}$-modes (i.e. a different quantization) yields a non-trivial w-factor in front of the derivative terms in the stress-tensor and therefore will correspond to a non-trivial red-shift physics for the system. Consequently, thermal-phases may appear as a result of this.[6] Note, however, that this is too crude to pass as an argument since we have not factored in the inequivalent conjugacy classes and we have also been imprecise about where the "red-shift" matters, i.e. near the origin of the complex plane or near infinity. Nonetheless, it raises an intriguing possibility of a more precise physical picture along these lines and we hope to address this in future.

---

[6]Qualitatively, this is similar to the Rindler-physics, although it appears more subtle and layered.

For holographic CFT's, it would be insightful to get a dual gravitational description of the dynamics. This can be done from two different perspectives: one that is based on the explicit time-dependent Hamiltonian and the other that is based on the Floquet Hamiltonian. While the former yields a dynamical geometry, the latter is capable of describing static "patches" of the geometry which correspond to the different phases (heating and non-heating) and the phase boundary. For the $1 + 1$ dimensional case, the dynamical scenario has been explored in [7–9], while the Floquet-Hamiltonian based approach is discussed in [22]. In [7], a non-trivial dynamical horizon structure has been observed, whereas the different geometric patches of [22] were obtained by solving integral curves that are generated by the (appropriate combination of) bulk Killing vector that is dual to the CFT Floquet Hamiltonian. Interestingly, the integral curve approach is also explored in a completely different context of "bulk reconstruction" in which a local bulk observer in an AdS-geometry is described in terms of the CFT Hamiltonian, see e.g. [36, 37],.

The higher dimensional generalization of the bulk geometric description is potentially very interesting. First, it is rather non-trivial to obtain horizons with structures in higher dimensional black holes. Secondly, it is also technically involved to obtain dynamical horizons, outside Vaidya-type geometries. Moreover, from the integral curve perspective, a local bulk observer seems readily describable in terms of the CFT Floquet Hamiltonian using the bulk Killing vectors that describe the $\mathrm{SL}(2, C)$ sub-algebra of the conformal algebra, see for example appendix C for explicit expressions of the corresponding generators. We are currently exploring this aspect in detail.

Let us now offer some comments that are not necessarily limited to CFTs. It is evident that the crucial ingredients of our results are the following: (i) The existence of an $\mathrm{SL}(2, C)$ algebra as a sub-algebra of the symmetry group of the system and (ii) a "quasi-primary" representation of the fields under this $\mathrm{SL}(2, C)$.[7] Interestingly, scattering matrix elements in $(3 + 1)$ and $(2 + 1)$-dimensions can be recast into correlation functions of quasi-primary operators at null infinity known as the celestial sphere, see e.g. [40–42] for explicit details on this. These quasi-primaries form the continuous principal series, $\Delta = \frac{d-1}{2} + is$, in $(d + 1)$-dimensions and s is real-valued; we have collected some relevant and explicit formulae in appendix D for a more direct comparison. Even though the "CFT-spectrum" is continuous and complex-valued, the corresponding correlators are real-valued since it involves both Δ and $\bar{\Delta}$. Thus, the presence of a heating and a non-heating phase along with a phase boundary is expected in this case as well. Note, however, that this entails a rather non-trivial quantization of the system: the Minkowski coordinates, X^μ, are first mapped to a stereographic coordinates on the null sphere, w; subsequently, the w-plane is mapped to the cylinder by $\zeta = \exp(2\pi w/L)$. Identifying $\zeta = T + ix$ and analytically continuing $T \to iT_L$ yields the Lorentzian system (with Lorentzian time T_L) for which the phases are expected to exist for different conjugacy classes of the $\mathrm{SL}(2, C)$-transformations. It will be very interesting to explore this aspect as well as its connection with scattering matrix physics in detail, which we leave for future.

---

[7]A similar statement holds for an $\mathrm{SL}(2, R)$ algebra as well.

Acknowledgments

A Transformation of the generators

In this section, we use infinitesimal coordinate transformations to obtain expressions of the generators in the deformed frame as eluded to in the main text. To this end, we recollect from the main text that the transformation of the generators D, K_0 and P_0 can be easily obtained as follows

$$U^{-1}\sigma_z U = \tau_z = \cosh\theta\sigma_z + \sinh\theta i\sigma_x$$
$$U^{-1}\sigma_x U = \tau_x = \cosh\theta\sigma_x - i\sigma_z\sinh\theta, \quad \tau_y = \sigma_y \tag{A.1}$$

where $U = \exp[-i\theta(K_0 - P_0)/2]$ as defined in the main text and the last relation follows from the fact that U commutes with σ_y. Eq. (A.1) therefore species the relations between the generators D, K_t and P_t and their deformed versions D', K_0' and P_0'. These are given by

$$D' = D\cosh\theta - \frac{1}{2}(K_0 + P_0)\sinh\theta$$
$$K_0'[P_0'] = \frac{1}{2}(1 + \cosh\theta)K_0[P_0] - \frac{1}{2}(1 - \cosh\theta)P_0[K_0] - D\sinh\theta \tag{A.2}$$

where we have used eq. (2.3) to obtain the generators from the Pauli matrices.

To construct rest of the transformed generators, we need to use their coordinate representation. For this, it is convenient to first consider an infinitesimal transformation $U_{\text{inf}} = 1 - i\theta(K_0 - P_0)/2$. The transformation of coordinates $(\tau, x, y, z) \equiv (\tau, x_j)$ under the action of U_{inf} can be computed and yields

$$\tau' = U\tau = \tau - \frac{\theta}{2}(1 + r^2 - 2\tau^2), \quad x_j' = Ux_j = x_j(1 + \theta\tau) \tag{A.3}$$

The reverse transformation expressing (τ, x_j) in terms of (τ', x_j') can be obtained from eq. (A.3) and yields

$$\tau = \tau' + \frac{\theta}{2}(1 + (r')^2 - 2\tau'^2), \quad x_j = x_j'(1 - \theta\tau') \tag{A.4}$$

We now use the transformed coordinates to write the expressions of the generators. For example, one finds

$$P_0' = -i\partial_{\tau'} = -i\partial_\tau + i\theta(\tau\partial_\tau + \sum_j x_j\partial_j) = P_0 - \theta D \tag{A.5}$$

where we have used eq. (A.4). Note that this coincides with the infinitesimal version of eq. (A.2) as expected; this can also be explicitly checked for D and K_0.

Next we find the other generators where the use of the transformed coordinates provides us the infinitesimal version of the generators in the deformed frame. For example, one finds

$$P'_j = -i\partial_{x'_j} = -i(\partial_{x_j} + \theta(x_j\partial_\tau - \tau\partial_{x_j})) = P_j + \theta L_{0j} \tag{A.6}$$

$$K'_j = -i(x'_j(\tau'\partial_{\tau'} + \sum_j x'_j\partial_{x'_j}) - (r')^2\partial_{x'_j})$$
$$= -i(x_j(\tau\partial_\tau + \sum_j x_j\partial_{x_j}) - r^2\partial_{x_j}) - i\theta(\tau\partial_{x_j} - x_j\partial_\tau) = K_j - \theta L_{0j} \tag{A.7}$$

where $L_{\mu\nu} = i(x_\mu\partial_{x_\nu} - x_\nu\partial_{x_\mu})$ are the angular momentum generators. A simlar analysis yields

$$L'_{0j} = L_{0j} + \frac{\theta}{2}(P_j - K_j), \quad L'_{ij} = L_{ij}. \tag{A.8}$$

It can be easily checked that the generators obtained in eqs. (A.6), (A.7), and (A.8), together with the infinitesimal version of D, K_0 and P_0 obtained from eq. (A.2), satisfy the conformal algebra to $O(\theta)$.

Next, we look for the transformed generators for finite conformal transformation. Instead of a direct calculation via coordinate transformations which is cumbersome, we use the results obtained for infinitesimal transformations and the criteria that these generators must satisfy the conformal algebra. It turns out that these two criteria can uniquely specify the deformed generators. To see this, we first consider P_j. Eq. (A.6) dictates the infinitesimal version of P'_j; taking cue from this and eq. (A.2), we write

$$P'_j = \frac{1}{2}(1 + \cosh\theta)P_j + \frac{1}{2}(1 - \cosh\theta)K_j + L_{0j}\sinh\theta \tag{A.9}$$

The first check to ensure that this is the correct form is to verify the commutator $[D', P_j] = iP'_j$. Written explicitly, using standard commutation relation of conformal generators, this yields

$$[D', P'_j] = i\left(\frac{\cosh\theta(1 + \cosh\theta)}{2}P_j - \frac{\cosh\theta(1 - \cosh\theta)}{2}K_j - \frac{1}{2}\sinh^2\theta(P_j + K_j)\right.$$
$$\left. + \sinh\theta L_{0j}\right) = iP'_j \tag{A.10}$$

Next, we need to check the commutation relation between P'_j and K'_j. For this one needs to know K'_j. Using eq. (A.7) and taking cue from the form of P'_j, we write

$$K'_j = \frac{1}{2}(1 + \cosh\theta)K_j + \frac{1}{2}(1 - \cosh\theta)P_j - L_{0j}\sinh\theta \tag{A.11}$$

This form ensures $[D', K'_j] = -iK'_j$ and this can be checked in a similar manner. The commutation of K'_j and P'_j can be computed to be

$$[K'_j, P'_j] = 2i\left(\frac{(1 + \cosh\theta)^2 - (1 - \cosh\theta)^2}{4}D - \sinh\theta(K_0 + P_0)\right) = 2iD' \tag{A.12}$$

The commutation of P_0' and K_j' can also be checked and yields

$$[K_j', P_0'] = 2i\left(\frac{(1+\cosh\theta)^2 - (1-\cosh\theta)^2}{4}L_{0j} + \frac{1}{2}\sinh\theta D(P_j - K_j)\right)$$
$$= 2i\left(\cosh\theta\, L_{0j} + \sinh\theta(P_j - K_j)/2\right) = 2iL_{0j}' \tag{A.13}$$

Note that the form of $L_{0j}' = \cosh\theta\, L_{0j} + \sinh\theta(P_j - K_j)/2$ so obtained is consistent with eq. (A.8). Further it can be checked that $[D', L_{0j}'] = 0$. The other commutation relations involving L_{ij}' and L_{0j}' also holds provided we set $L_{ij}' = L_{ij}$. Thus the final expressions of the deformed generators, used in the main text, are given by

$$D' = D\cosh\theta - \frac{1}{2}(K_0 + P_0)\sinh\theta$$
$$K_0' = \frac{1}{2}(1+\cosh\theta)K_0 - \frac{1}{2}(1-\cosh\theta)P_0 - D\sinh\theta$$
$$P_0' = \frac{1}{2}(1+\cosh\theta)P_0 - \frac{1}{2}(1-\cosh\theta)K_0 - D\sinh\theta$$
$$K_j' = \frac{1}{2}(1+\cosh\theta)K_j + \frac{1}{2}(1-\cosh\theta)P_j - L_{0j}\sinh\theta$$
$$P_j' = \frac{1}{2}(1+\cosh\theta)P_j + \frac{1}{2}(1-\cosh\theta)K_j + L_{0j}\sinh\theta$$
$$L_{0j}' = \cosh\theta\, L_{0j} + \frac{1}{2}\sinh\theta(P_j - K_j), \quad L_{ij}' = L_{ij} \tag{A.14}$$

Thus eq. (A.14) provides a complete description of the deformed CFT in terms of the new generators.

B Coordinate transformation involving different subgroups

In this subsection, we provide an alternative formulation for coordinate transformation involving different SU(1, 1) subgroups. To this end we define the initial quaternion matrix to be

$$Q = x_\mu I - i(\sigma_i x_\nu + \sigma_j x_\lambda + \sigma_k x_\delta) \tag{B.1}$$

where $\sigma_{i,j,k}$ denote Pauli matrices with $\sigma_j\sigma_k = -i\sigma_i$, I is the 2×2 identity matrix, and $\mu \neq \nu, \lambda, \delta$.

Next we consider a transformation involving D, K_ν, and P_ν, where $\nu \neq \mu$. Let us consider a evolution operator $\mathrm{U}(T, 0)$ constructed using D, K_ν and P_ν given by

$$U_\nu = \begin{pmatrix} \tilde{a}_\nu & \tilde{b}_\nu \\ \tilde{c}_\nu & \tilde{d}_\nu \end{pmatrix} \tag{B.2}$$

where $\tilde{a}_\nu\tilde{d}_\nu - \tilde{b}_\nu\tilde{c}_\nu = 1$. We consider a quaternion matrix Q' which can be written as

$$Q' = x_\nu I - i(\sigma_i x_\mu + \sigma_j x_\delta + \sigma_k x_\lambda). \tag{B.3}$$

In this frame, the transformation of coordinates is known to be

$$Q_{\text{new}} = (\tilde{a}_\nu Q' - i\tilde{b}_\nu I).(i\tilde{c}_\nu Q' + \tilde{d}_\nu I)^{-1} \tag{B.4}$$

To obtain from Q_{new} starting from Q (eq. (B.1)), we therefore need to transform Q to Q'. This can be done by noting that

$$Q' = \sigma_j Q \sigma_k \tag{B.5}$$

where we have used $\sigma_j \sigma_k = -i\sigma_i$. Substituting eq. (B.5) in eq. (B.4) we find

$$Q_{\text{new}} = (AQ - iB).(iCQ + D)^{-1} \tag{B.6}$$
$$A = \tilde{a}_\nu \sigma_j, \quad B = \tilde{b}_\nu \sigma_k$$
$$C = \tilde{c}_\nu \sigma_j, \quad D = \tilde{d}_\nu \sigma_k$$

The above transformations indicate that a square-pulse protocol involving different SU(1,1) subgroups do not have a SU(1,1) valued U(T,0); this can be seen by noting that one needs to carry out intermediate basis changes to find the final coordinate when the transformation involves different U_μ (as in eqs. (4.4) and (4.6) of section 4.1) and a simple matrix product involving different U_μ does not yield the correct coordinate transformation. Our analysis here also demonstrates that the arrangement of coordinates in the initial quaternion matrix Q may be done arbitrarily without affecting the final result as eluded to in section 3.1

C Conformal algebra in *d*-dimensions

In this appendix, for completeness, we briefly collect the well-known conformal algebra and the corresponding generators. We will closely follow the notations of [39]. The conformal algebra in R^d is given by the SO($d+1,1$) algebra, with the following commutation relations:

$$[D, P_\mu] = iP_\mu, \quad [D, K_\mu] = -iK_\mu, \quad [K_\mu, P_\nu] = 2i(\delta_{\mu\nu}D - M_{\mu\nu}), \tag{C.1}$$

$$[M_{\mu\nu}, P_\alpha] = i(\delta_{\nu\alpha}P_\mu - \delta_{\mu\alpha}P_\nu), \quad [M_{\mu\nu}, K_\alpha] = i(\delta_{\nu\alpha}K_\mu - \delta_{\mu\alpha}K_\nu), \tag{C.2}$$

$$[M_{\alpha\beta}, M_{\mu\nu}] = i(\delta_{\alpha\mu}M_{\beta\nu} + \delta_{\beta\nu}M_{\alpha\mu} - \delta_{\beta\mu}M_{\alpha\nu} - \delta_{\alpha\nu}M_{\beta\mu}). \tag{C.3}$$

The differential operator representation of this algebra is given by

$$P_\mu = -i\partial_\mu, \quad D = -ix^\mu \partial_\mu, \quad M_{\mu\nu} = -i(x_\mu \partial_\nu - x_\nu \partial_\mu), \tag{C.4}$$

$$K_\mu = -2ix_\mu x^\nu \partial_\nu + ix^2 \partial_\mu. \tag{C.5}$$

The corresponding Euclidean AdS spacetime can be described by the hyperboloid in $R^{d+1,1}$:

$$-(X^0)^2 + (X^1)^2 + \ldots (X^{d+1})^2 = -L^2. \tag{C.6}$$

In the global patch, the AdS metric is given by

$$ds^2 = L^2 \left(\cosh^2 \rho \, d\tau^2 + d\rho^2 + \sinh^2 \rho \, dY_{d-1}^2 \right), \quad Y \cdot Y = 1. \tag{C.7}$$

The SO($d+1,1$) algebra is generated by the following Killing vectors in global coordinate:

$$D = -i\partial_\tau, \quad M_{\mu\nu} = -i\left(Y_\mu \frac{\partial}{\partial Y^\nu} - Y_\nu \frac{\partial}{\partial Y^\mu} \right),$$

$$P_\mu = -ie^{-\tau}\left[Y_\mu(\partial_\rho + \tanh \rho \, \partial_\tau) + \frac{1}{\tanh \rho}\nabla_\mu \right], \quad \nabla_\mu = \frac{\partial}{\partial Y^\mu} - Y_\mu Y^\nu \frac{\partial}{\partial Y^\nu},$$

$$K_\mu = -ie^{\tau}\left[Y_\mu(-\partial_\rho + \tanh \rho \, \partial_\tau) - \frac{1}{\tanh \rho}\nabla_\mu \right]. \tag{C.8}$$

One can check that on the boundary $\rho = \infty$ these Killing vectors generate via eq. (1.3) the Lüscher-Mack term $K_\mu + P_\mu$.

D SL(2, C), quasi-primaries, Lorentz symmetry

In this appendix we collect some relevant formulae and basic statements regarding the $\mathrm{SL}(2, C)$ action of the Lorentz group in $(3 + 1)$-dimensions. We will closely follow [40–43]. It is well-known that given a four-vector X^μ, we can associate a hermitian matrix:

$$X = \begin{bmatrix} X^0 - X^3 & X^1 + iX^2 \\ X^1 - iX^2 & X^0 + X^3 \end{bmatrix}, \quad \det(X) = -X^\mu X_\mu. \tag{D.1}$$

Now, an $\mathrm{SL}(2, C)$ matrix Θ acts on the hermitian matrix X as:

$$X' = \Theta X \Theta^\dagger, \quad \Theta = \begin{bmatrix} a & b \\ c & d \end{bmatrix}, \quad \text{with} \quad ad - bc = 1, \tag{D.2}$$

such that $\det(X') = \det(X)$.[8]

A more detailed action can be obtained by noting that the Lorentz group in $(3 + 1)$-dimensions acts as the global conformal group on the celestial sphere at infinity. More explicitly, given the Minkowski coordinates X^μ, $\mu = 0, \ldots 3$, the celestial sphere is defined by $\eta_{\mu\nu} X^\mu X^\mu = 0$, on which we can define: $w = (X^1 + iX^2)/(X^0 + iX^3)$. Under a Lorentz transformation: $X'^\mu = \Lambda^\mu_\nu X^\nu$, we get: $w' = (aw + b)/(cw + d)$, where $ad - bc = 1$ and a, b, c, d are complex-valued. Subsequently, the $(3 + 1)$-dimensional scattering amplitudes can be expressed as celestial CFT correlators.

For an explicit realization, [40–42] has defined quasi-primary fields under this $\mathrm{SL}(2, C)$ in the principal series, with a conformal dimension $\Delta = 1 + is$, where s is real-valued.[9] Moreover, there is a precise state-operator correspondence as well. The states are described by $\left| h, \bar{h}, w, \bar{w} \right\rangle$ where $\{w, \bar{w}\}$ are the stereographic coordinates of the celestial sphere. Lorentz transformation, denoted by $\mathrm{U}(\Lambda)$ acts on these states as follows:

$$\mathrm{U}(\Lambda) \left| h, \bar{h}, w, \bar{w} \right\rangle = \frac{1}{(cw + d)^h} \frac{1}{(\bar{c}\bar{w} + \bar{d})^{\bar{h}}} \left| h, \bar{h}, \frac{aw + b}{cw + d}, \frac{\bar{a}\bar{w} + \bar{b}}{\bar{c}\bar{w} + \bar{d}} \right\rangle, \tag{D.3}$$

$$\Lambda \in \mathrm{SL}(2, C), \quad h = \frac{1 + is - \sigma}{2}, \quad \bar{h} = \frac{1 + is + \sigma}{2}, \tag{D.4}$$

where σ denotes the helicity of the massless particle.

The corresponding basis quasi-primary states are given by

$$|s, \sigma, w = 0 = \bar{w}\rangle = \frac{1}{\sqrt{8\pi^4}} \int_0^\infty dE\, E^{is} |E, 0, 0, E, \sigma\rangle, \tag{D.5}$$

---

[8]In $(2 + 1)$-dimensions a similar description holds for a real-symmetric matrix [43]:

$$X = \begin{bmatrix} X^0 - X^2 & X^1 \\ X^1 & X^0 + X^2 \end{bmatrix}, \quad X' = \Lambda X \Lambda^T, \quad \Lambda \in \mathrm{SL}(2, R).$$

[9]In $(d + 1)$-dimensions, the corresponding conformal dimensions are $\Delta = \frac{d-1}{2} + is$.

such that the states are normalized as follows:

$$\langle s_1, \sigma_1, w_1, \bar{w}_1 | s_2, \sigma_2, w_2, \bar{w}_2 \rangle = \delta\left(s_1 - s_2\right) \delta^{(2)}\left(w_1 - w_2\right) \delta_{\sigma_1 \sigma_2}, \tag{D.6}$$

where

$$|s, \sigma, w, \bar{w}\rangle = \left(\frac{1}{1 + w\bar{w}}\right)^{1+is} \mathrm{U}\left(R(w, \bar{w})\right) |s, \sigma, 0, 0\rangle, \tag{D.7}$$

in which $\mathrm{U}\left(R(w, \bar{w})\right)$ are the unitary rotation operators. The action of the Lorentz group on these states then yields equation (D.3), which essentially is comprised of $\mathrm{SL}(2, C)$ matrix multiplications. The corresponding operators, denoted by $\mathcal{O}_{h, \bar{h}}$ will evolve in the Heisenberg picture according to:

$$\mathrm{U}(\Lambda)\mathcal{O}_{h, \bar{h}}\left(w, \bar{w}\right)\mathrm{U}(\Lambda)^\dagger = \left(\frac{\partial \Lambda w}{\partial w}\right)^h \left(\frac{\partial \Lambda \bar{w}}{\partial \bar{w}}\right)^{\bar{h}} \mathcal{O}_{h, \bar{h}}\left(\Lambda w, \Lambda \bar{w}\right). \tag{D.8}$$

A very similar description exists in $(2 + 1)$-dimensions as well, we refer the interested Reader to e.g. [43] for more details on this.

E Fixed points and trajectories for a single SU(1, 1) subgroup

For transformations which involve the subalgebra formed by D, K_0, P_0, one can choose

$$Q = x_0 I - i \sum_{i=1}^3 \sigma_i x_i \tag{E.1}$$

so that the transformations on R^4 become (3.8) with the entries a_i real numbers satisfying (3.9). In the following we will use the notation

$$\tilde{a} = \tilde{a}_1 \qquad \tilde{b} = i\tilde{a}_2 \qquad \tilde{c} = i\tilde{a}_3 \qquad \tilde{d} = \tilde{a}_4 \tag{E.2}$$

so that the transformation is

$$Q' = (\tilde{a}Q + \tilde{b})(\tilde{c}Q + \tilde{d})^{-1} \tag{E.3}$$

A fixed point $\bar{Q}$ satisfies

$$\bar{Q}(\tilde{c}\bar{Q} + \tilde{d}) = \tilde{a}\bar{Q} + \tilde{b} \qquad \tilde{a}\tilde{d} - \tilde{b}\tilde{c} = 1 \tag{E.4}$$

Using (E.4) and standard properties of the Pauli matrices it is then easy to see that there are three kinds of fixed points or surfaces.

1. $\bar{Q}^\pm = \bar{x}_0^\pm I$, i.e. $\bar{x}_i = 0$. Here

$$\bar{x}_0^\pm = \frac{1}{2\tilde{c}}\left[(\tilde{a} - \tilde{d}) \pm \sqrt{(\tilde{a} + \tilde{d})^2 - 4}\right] \tag{E.5}$$

In deriving (E.5) we have used (E.3). These are two fixed points and requires

$$(\tilde{a} + \tilde{d})^2 > 4 \tag{E.6}$$

The corresponding matrix

$$\begin{bmatrix} \tilde{a} & \tilde{b} \\ \tilde{c} & \tilde{d} \end{bmatrix} \tag{E.7}$$

is in the hyperbolic conjugacy class.

2. When $(\tilde{a} + \tilde{d})^2 < 4$ there is a fixed two dimensional hypersurface defined by

$$\bar{x}_0 = \frac{\tilde{a} - \tilde{d}}{2\tilde{c}} \qquad \sum_{i=1}^{3}(\bar{x}_i)^2 = \frac{1}{4\tilde{c}^2}\left(4 - (\tilde{a} + \tilde{d})^2\right) \tag{E.8}$$

and now the matrix in (E.7) is in the elliptic conjugacy class.

3. The case $(\tilde{a} + \tilde{d})^2 = 4$ is marginal and corresponds to the parabolic conjugacy class.

It is now straightforward to see that the transformation (E.3) can be re-expressed in the following form for hyperbolic and elliptic transformations:

$$(Q' - \bar{Q}^+)(Q' - \bar{Q}^-)^{-1} = (\tilde{c}\bar{Q}^- + \tilde{d})(Q - \bar{Q}^+)(Q - \bar{Q}^-)^{-1}(\tilde{c}\bar{Q}^+ + \tilde{d})^{-1} \tag{E.9}$$

For the elliptic conjugacy class, the $\bar{Q}^{\pm}$ in this equation refer to two antipodal points on the fixed 2-surface defined in (E.8).

To prove (E.9) we substitute (E.3) in the left hand side of this equation so that the left hand side becomes

$$\left[(\tilde{a} - \tilde{c}\bar{Q}^+)Q + (\tilde{b} - \tilde{d}\bar{Q}^+)\right]\left[(\tilde{a} - \tilde{c}\bar{Q}^-)Q + (\tilde{b} - \tilde{d}\bar{Q}^-)\right]^{-1} \tag{E.10}$$

while the right hand side of (E.9) becomes

$$\left[(\tilde{c}\bar{Q}^- + \tilde{d})Q - (\tilde{c}\bar{Q}^- + \tilde{d})\bar{Q}^+\right]\left[(\tilde{c}\bar{Q}^+ + \tilde{d})Q - (\tilde{c}\bar{Q}^+ + \tilde{d})\bar{Q}^-\right]^{-1} \tag{E.11}$$

For the hyperbolic case, $\bar{Q}^{\pm}$ are both proportional to the identity matrix. For the elliptic case, we can take the antipodal points on the fixed 2-surface to be along the 3 axis without any loss of generality. For both these cases one can then explicitly check that

$$\bar{Q}^+ + \bar{Q}^- = \frac{\tilde{a} - \tilde{d}}{\tilde{c}} \cdot I \qquad \bar{Q}^+\bar{Q}^- = \bar{Q}^-\bar{Q}^+ = -\frac{\tilde{b}}{\tilde{c}} \cdot I \tag{E.12}$$

Using these relations and the relation (E.4) it may be checked that (E.10) and (E.11) are equal term by term.

The relationship (E.3) can be iterated to yield

$$Q'^{(n)} = \left(I - (\tilde{c}Q_- + \tilde{d})^n \alpha_{\pm}(Q)(\tilde{c}Q_+ + \tilde{d})^{-n}\right)^{-1}\left(Q_+ - \left((\tilde{c}Q_- + \tilde{d})^n \alpha_{\pm}(Q)(\tilde{c}Q_+ + \tilde{d})^{-n}\right)Q_-\right), \tag{E.13}$$

where

$$\alpha_{\pm}(Q) = \left[(Q - Q_+)(Q - Q_-)^{-1}\right].$$

which can be used to determine the trajectory of a point under successive transformations.

The Euclidean distance between two points represented by quaternions Q_1 and Q_2 are given by $\sqrt{|\mathrm{Det}(Q_1 - Q_2)|}$. Equation (E.9) implies

$$\frac{\mathrm{Det}(Q' - \bar{Q}^+)}{\mathrm{Det}(Q' - \bar{Q}^-)} = R^2 \frac{\mathrm{Det}(Q - \bar{Q}^+)}{\mathrm{Det}(Q - \bar{Q}^-)} \tag{E.14}$$

where

$$R^2 = \frac{\mathrm{Det}(\tilde{c}Q^- + \tilde{d})}{\mathrm{Det}(\tilde{c}Q^+ + \tilde{d})} = \left(\frac{\tilde{a} + \tilde{d} - \sqrt{(\tilde{a} + \tilde{d})^2 - 4}}{\tilde{a} + \tilde{d} + \sqrt{(\tilde{a} + \tilde{d})^2 - 4}} \right)^2 \qquad \text{(Hyperbolic)}$$

$$R^2 = 1 \qquad\qquad\qquad \text{(Elliptic)} \tag{E.15}$$

The equation can be recursively applied to yield

$$\frac{\mathrm{Det}(Q^{(n)} - \bar{Q}^+)}{\mathrm{Det}(Q^{(n)} - \bar{Q}^+)} = R^{2n} \frac{\mathrm{Det}(Q - \bar{Q}^+)}{\mathrm{Det}(Q - \bar{Q}^+)} \tag{E.16}$$

where Q^n denotes the transformed point after n such transformations. The expressions for R^2 then immediately implies that for hyperbolic transformations a point converges to one of the fixed points for large n, whereas for ellipic transformations, the point keeps moving on a circle of fixed radius around a point on the fixed surface. Note that when we analytically continue to Lorentzian times we end up with $a = d^*$ which keeps the combination $a + d$ real. Hence we can classify dynamics based on if R^2 is a pure phase or real. This corresponds to $\mathrm{Re}(a)$ being either less than 1 or greater.

Using the relation (E.13) we can calculate various physical quantities under a Floquet drive of this type, after n cycles. The result depends on the conjugacy class of the transformation at the end of a cycle. However the general features will be similar to the $d = 1$ case, i.e. hyperbolic classes lead to a heating phase while elliptic classes lead to oscillatory phase [12, 14, 16].

When a cycle involves two different $\mathrm{SL}(2, R)$ subgroups of the conformal group, e.g. two different Π_μ's, one can no longer represent the net transformation by a $\mathrm{SL}(2, H)$ transformation with parameters proportional to the identity, rather a change is basis in required, see appendix section B.The analysis of fixed points (surfaces) etc. needs to be re-done by investigating the conjugacy invariants of $\mathrm{SL}(2, H)$ [35], and the result of such Floquet drives will be quite different. Explicit results for physical quantities under Floquet dynamics will appear in a future publication.

References

[1] A. Polkovnikov, K. Sengupta, A. Silva and M. Vengalattore, *Nonequilibrium dynamics of closed interacting quantum systems*, *Rev. Mod. Phys.* **83** (2011) 863 [`arXiv:1007.5331`] [InSPIRE].

[2] L. D'Alessio, Y. Kafri, A. Polkovnikov and M. Rigol, *From quantum chaos and eigenstate thermalization to statistical mechanics and thermodynamics*, *Adv. Phys.* **65** (2016) 239 [`arXiv:1509.06411`] [InSPIRE].

[3] M. Bukov, L. D'Alessio and A. Polkovnikov, *Universal high-frequency behavior of periodically driven systems: from dynamical stabilization to Floquet engineering*, *Adv. Phys.* **64** (2015) 139.

[4] A. Sen, D. Sen and K. Sengupta, *Analytic approaches to periodically driven closed quantum systems: methods and applications*, *J. Phys. Condens. Matter* **33** (2021) 443003 [`arXiv:2102.00793`] [InSPIRE].

[5] P. Calabrese and J. Cardy, *Entanglement and correlation functions following a local quench: a conformal field theory approach*, *J. Stat. Mech.* **0710** (2007) P10004 [arXiv:0708.3750] [INSPIRE].

[6] X. Wen and J.-Q. Wu, *Quantum dynamics in sine-square deformed conformal field theory: Quench from uniform to nonuniform conformal field theory*, *Phys. Rev. B* **97** (2018) 184309 [arXiv:1802.07765] [INSPIRE].

[7] K. Goto et al., *Non-Equilibrating a Black Hole with Inhomogeneous Quantum Quench*, arXiv:2112.14388 [INSPIRE].

[8] K. Goto et al., *Scrambling and recovery of quantum information in inhomogeneous quenches in two-dimensional conformal field theories*, *Phys. Rev. Res.* **6** (2024) 023001 [arXiv:2302.08009] [INSPIRE].

[9] J. Kudler-Flam et al., *Bridging two quantum quench problems — local joining quantum quench and Möbius quench — and their holographic dual descriptions*, *JHEP* **08** (2024) 213 [arXiv:2309.04665] [INSPIRE].

[10] K. Goto et al., *Spatial deformation of many-body quantum chaotic systems and quantum information scrambling*, *Phys. Rev. B* **109** (2024) 054301 [arXiv:2305.01019] [INSPIRE].

[11] M. Nozaki, K. Tamaoka and M.T. Tan, *Inhomogeneous quenches as state preparation in two-dimensional conformal field theories*, *Phys. Rev. D* **109** (2024) 126014 [arXiv:2310.19376] [INSPIRE].

[12] X. Wen and J.-Q. Wu, *Floquet conformal field theory*, arXiv:1805.00031 [INSPIRE].

[13] B. Lapierre et al., *Emergent black hole dynamics in critical Floquet systems*, *Phys. Rev. Res.* **2** (2020) 023085 [arXiv:1909.08618] [INSPIRE].

[14] X. Wen, R. Fan, A. Vishwanath and Y. Gu, *Periodically, quasiperiodically, and randomly driven conformal field theories*, *Phys. Rev. Res.* **3** (2021) 023044 [arXiv:2006.10072] [INSPIRE].

[15] R. Fan, Y. Gu, A. Vishwanath and X. Wen, *Floquet conformal field theories with generally deformed Hamiltonians*, *SciPost Phys.* **10** (2021) 049 [arXiv:2011.09491] [INSPIRE].

[16] D. Das, R. Ghosh and K. Sengupta, *Conformal Floquet dynamics with a continuous drive protocol*, *JHEP* **05** (2021) 172 [arXiv:2101.04140] [INSPIRE].

[17] N. Ishibashi and T. Tada, *Dipolar quantization and the infinite circumference limit of two-dimensional conformal field theories*, *Int. J. Mod. Phys. A* **31** (2016) 1650170 [arXiv:1602.01190] [INSPIRE].

[18] T. Tada, *Sine-Square Deformation and its Relevance to String Theory*, *Mod. Phys. Lett. A* **30** (2015) 1550092 [arXiv:1404.6343] [INSPIRE].

[19] K. Okunishi, *Sine-square deformation and Möbius quantization of 2D conformal field theory*, *PTEP* **2016** (2016) 063A02 [arXiv:1603.09543] [INSPIRE].

[20] T. Tada, *Conformal Quantum Mechanics and Sine-Square Deformation*, *PTEP* **2018** (2018) 061B01 [arXiv:1712.09823] [INSPIRE].

[21] P. Caputa and I. MacCormack, *Geometry and Complexity of Path Integrals in Inhomogeneous CFTs*, *JHEP* **01** (2021) 027 [*Erratum ibid.* **09** (2022) 109] [arXiv:2004.04698] [INSPIRE].

[22] S. Das et al., *Brane detectors of a dynamical phase transition in a driven CFT*, *SciPost Phys.* **15** (2023) 202 [arXiv:2212.04201] [INSPIRE].

[23] S.R. Das, D.A. Galante and R.C. Myers, *Smooth and fast versus instantaneous quenches in quantum field theory*, *JHEP* **08** (2015) 073 [arXiv:1505.05224] [INSPIRE].

[24] A. Dymarsky and M. Smolkin, *Universality of fast quenches from the conformal perturbation theory*, *JHEP* **01** (2018) 112 [`arXiv:1709.08654`] [ɪɴSPIRE].

[25] Y. Chen, V. Ivo and J. Maldacena, *Comments on the double cone wormhole*, *JHEP* **04** (2024) 124 [`arXiv:2310.11617`] [ɪɴSPIRE].

[26] D. Martínez-Tibaduiza, A.H. Aragão, C. Farina and C.A.D. Zarro, *New BCH-like relations of the su(1,1), su(2) and so(2,1) Lie algebras*, *Phys. Lett. A* **384** (2020) 126937 [`arXiv:2005.09500`] [ɪɴSPIRE].

[27] V.K. Dobrev et al., *Harmonic Analysis on the n-Dimensional Lorentz Group and Its Application to Conformal Quantum Field Theory*, Springer Berlin, Heidelberg (1977) [`DOI:10.1007/BFb0009678`] [ɪɴSPIRE].

[28] V.K. Dobrev and V.B. Petkova, *Elementary Representations and Intertwining Operators for the Group SU*(4)*, *Rept. Math. Phys.* **13** (1978) 233 [ɪɴSPIRE].

[29] J.B. Wilker, *The quaternion formalism for Möbius groups in four or fewer dimensions*, *Linear Algebra Appl.* **190** (1993) 99.

[30] A. Pal and K. Ray, *Conformal Correlation functions in four dimensions from Quaternionic Lauricella system*, *Nucl. Phys. B* **968** (2021) 115433 [`arXiv:2005.12523`] [ɪɴSPIRE].

[31] D. Simmons-Duffin, *The Conformal Bootstrap*, in the proceedings of the *Theoretical Advanced Study Institute in Elementary Particle Physics: New Frontiers in Fields and Strings*, Boulder, U.S.A., June 01–26 (2015) [`DOI:10.1142/9789813149441_0001`] [`arXiv:1602.07982`] [ɪɴSPIRE].

[32] E.M. Brehm and M. Broccoli, *Correlation functions and quantum measures of descendant states*, *JHEP* **04** (2021) 227 [`arXiv:2012.11255`] [ɪɴSPIRE].

[33] R. Fan, Y. Gu, A. Vishwanath and X. Wen, *Emergent Spatial Structure and Entanglement Localization in Floquet Conformal Field Theory*, *Phys. Rev. X* **10** (2020) 031036 [`arXiv:1908.05289`] [ɪɴSPIRE].

[34] J.P. Marco Meineri, In *Conformal Field Theory and Gravity EPFL doctoral course*, (2019) [https://www.epfl.ch/labs/fsl/wp-content/uploads/2022/05/CFTandGravity.pdf]

[35] B. Foreman, *Conjugacy invariants of Sl(2,H)*, *Linear Algebra Appl.* **381** (2004) 25.

[36] D.L. Jafferis and L. Lamprou, *Inside the hologram: reconstructing the bulk observer's experience*, *JHEP* **03** (2022) 084 [`arXiv:2009.04476`] [ɪɴSPIRE].

[37] E. Bahiru et al., *State-dressed local operators in the AdS/CFT correspondence*, *Phys. Rev. D* **108** (2023) 086035 [`arXiv:2209.06845`] [ɪɴSPIRE].

[38] A. Dymarsky and K. Pavlenko, *Generalized Eigenstate Thermalization Hypothesis in 2D Conformal Field Theories*, *Phys. Rev. Lett.* **123** (2019) 111602 [`arXiv:1903.03559`] [ɪɴSPIRE].

[39] P. Di Francesco, P. Mathieu and D. Sénéchal, *Conformal Field Theory*, Springer New York (1997) [`DOI:10.1007/978-1-4612-2256-9`].

[40] S. Pasterski, S.-H. Shao and A. Strominger, *Flat Space Amplitudes and Conformal Symmetry of the Celestial Sphere*, *Phys. Rev. D* **96** (2017) 065026 [`arXiv:1701.00049`] [ɪɴSPIRE].

[41] S. Pasterski and S.-H. Shao, *Conformal basis for flat space amplitudes*, *Phys. Rev. D* **96** (2017) 065022 [`arXiv:1705.01027`] [ɪɴSPIRE].

[42] E. Crawley, N. Miller, S.A. Narayanan and A. Strominger, *State-operator correspondence in celestial conformal field theory*, *JHEP* **09** (2021) 132 [`arXiv:2105.00331`] [ɪɴSPIRE].

[43] S. Banerjee, *Null Infinity and Unitary Representation of The Poincare Group*, *JHEP* **01** (2019) 205 [`arXiv:1801.10171`] [ɪɴSPIRE].